ΠΟΛΥΤΕΧΝΕΙΟ ΚΡΗΤΗΣ

Σχολή Ηλεκτρολόγων Μηχανικών και Μηχανικών Υπολογιστών

Spectral Chromatometry

Diploma Thesis - Bousias Dimitris

Φασματική Χρωματομετρία

Διπλωματική Εργασία

του φοιτητή

Μπούσια Δημήτρη

Εξεταστική Επιτροπή:

Μπάλας Κωσταντίνος (επιβλέπων)

Ζερβάκης Μιχάλης

Κορτσαλιουδάκης Ναθαναήλ

Acknowledgements

I wish to express my honest gratitude to my Professors for their inspiration, their guidance, motivating knowledge, insight as well as the challenges they posed on me to overcome. Without them this thesis would have never come into fruition. Their paradigm and work are a great road to follow and to strive upon.

I would like to thank my lab-mates and members of the Electronics Laboratory for their valuable comments, observations and encouragement, and for all the fun we have had all this time.

This thesis is dedicated to my family and friends, for their love ,trust, and understanding, that shaped me into who I am.

Abstract

Scientific breakthroughs and technological advancement help us see and understand the world around us better. The field of spectroscopy and the technology behind it exist for the same reason too. They allow us to see the unseen, expand and improve the human vision, our major mechanism in understanding the world and our presence in it.

Color is an interpretation of our environment but is not completely revealing by itself of the deeper 'truths' that help form it, such as the interaction of light with matter.

In this thesis we study how color stimulus is formed and research how we can optimally reproduce it. Spectroscopic measurements were performed to determine the spectral reflectances of Colorimetric charts, standards in the color science world. Various common and scientific light sources are measured to determine their Spectral Power Distribution, which can be used as a tool for detecting the illumination in unknown conditions. A practical Snapshot Multispectral method is described, and used to produce high fidelity color results of scenes, regardless of the illumination. We elaborate on how to overcome problems inherent to the color production such as metamerism.

Table of Contents

Introduction

Theoretical background and concept definitions

Color

Color is a visual perceptual property, defined as the quality of an object or substance with respect to the light reflected, emitted or transmitted by it. Color derives from the spectrum of light(distribution of light power versus wavelength or frequency)interacting in the eye with the spectral sensitivities of the light receptors. Although it can be measured and quantified in various ways, the perception of it is a subjective process since different people or organisms can see the same illuminated object or light source in different ways.[1]

Light - Electromagnetic Radiation

Light is electromagnetic(EM) radiation, the fluctuations of electric and magnetic fields in nature.

The human eye is only sensitive to EM radiation at wavelengths that range roughly between 380 nanometers and 780 nanometers. This segment is what we call the visible spectrum or visible light. Infrared lies just above red light; ultraviolet exists just below violet light. Both are invisible to humans and most creatures.

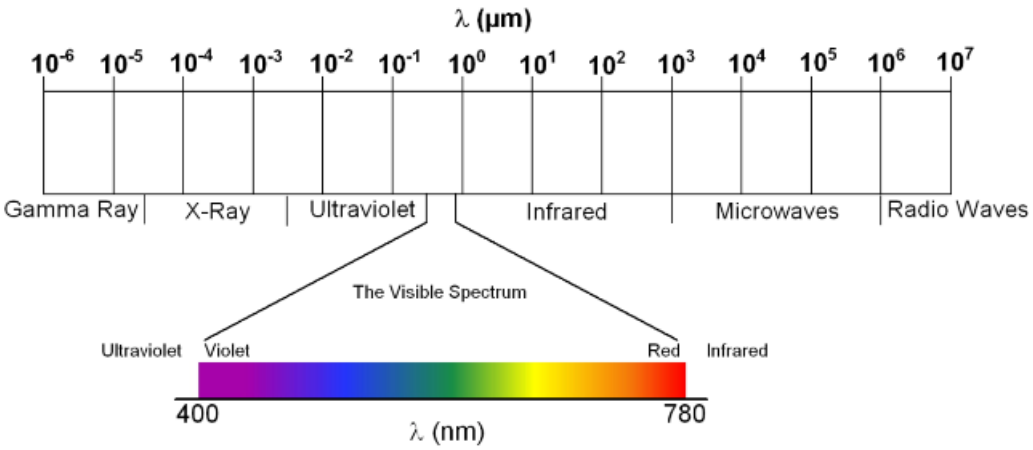

Fig.1: The visible spectrum, its range in wavelength and its composition of pure spectral or monochromatic colors , six of which (violet, blue, green, yellow, orange, red) are known as Newtonian colors The spectrum is continuous, without clear boundaries, between one color and the next.

The visible spectrum contains numerous colors that are distinguished by wavelength and amplitude; wavelength determines color and amplitude determines brightness.[2]

The Human Eye

Perception of color begins with specialized retinal cells containing pigments with different spectral sensitivities, known as cone cells. The human eye(one of the most complex visual sensory organs) contains three types of those cones, which are located in the fovea, a central part of the retina . The receptors contain different variations of the protein photopsin causing differences in the optimum wavelength absorbed.

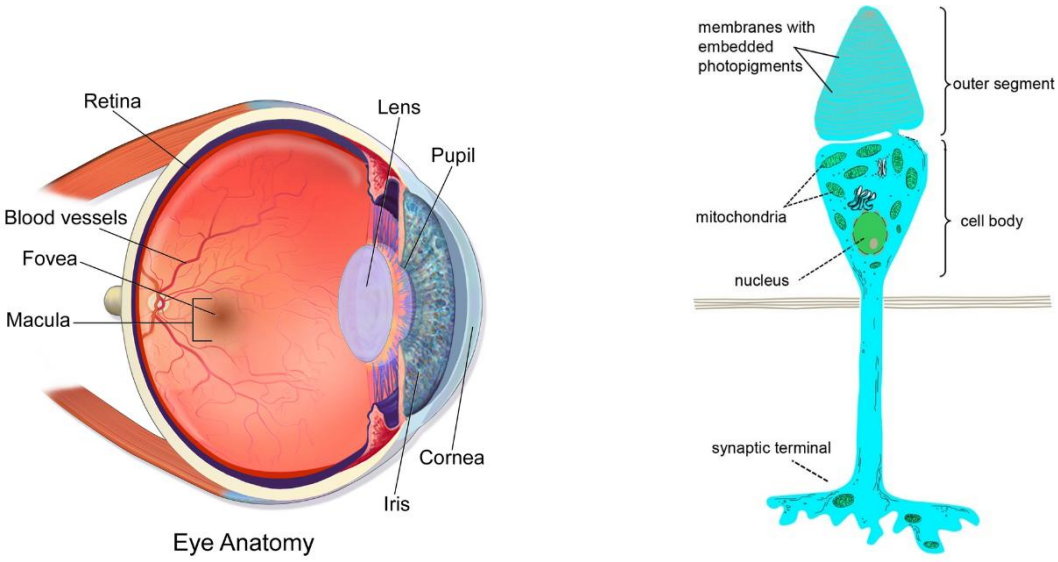

Fig.2 The anatomy of the human eye, and the photoreceptive cone cell

The three types of cones are responsive to light with wavelengths peaking at around 430 nm , 540 nm, and 570 nm varying for each individual and are called S, M , L cones respectively (abbreviations for Short , Medium and Long wavelengths).

Light, no matter how complex its composition of wavelengths, is reduced to three color components by the eye. For each location in the visual field, the three types of cones yield three signals based on the extent to which each is stimulated. These amounts of stimulation are usually called **tristimulus values**.[3]

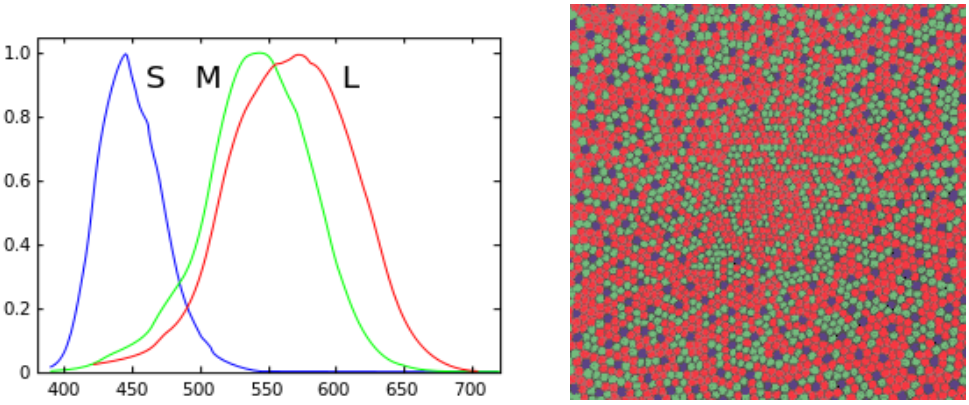

Fig.3: (a) Normalized responsivity spectra of human cone cells, S, M, and L types. (b) Distribution of cone cells in the retinal fovea

The response curve as a function of wavelength varies for each type of cone. Because the curves overlap (as can be seen in Fig.3.a), there exist some tristimulus values that cannot occur for any incoming light combination. It is estimated that the average human can distinguish up to ten million different colors.[4][5]

Reflectance

In order to understand why different objects appear with different color we must describe the way said objects react to incident light. As a light source with its characteristic spectral power distribution illuminates a surface part of that illumination might be absorbed by the material while another part reflected(both by a factor).The effectiveness with which said material reflects radiant light is its Reflectance. It is a property *highly correlated with the chemical composition and the molecular structure of a material*. When Reflectance is plotted as a function of wavelength the result is the spectral reflectance curve, where one can notice and analyze the spectral reflectance patterns or **spectral signatures** of different materials.[6]

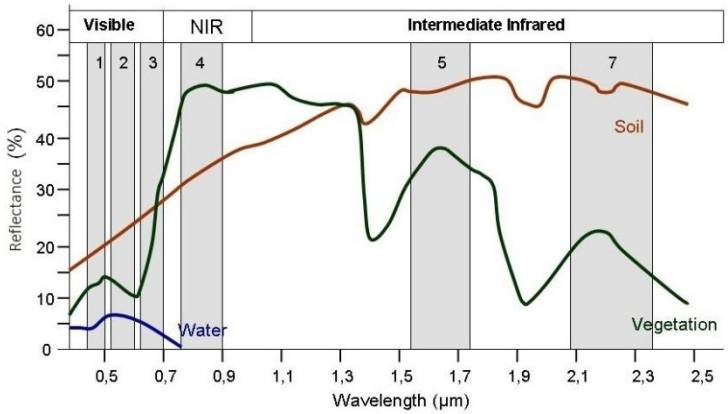

Fig.4: Spectral signatures of soil, vegetation and water

Reflectance as a property of a surface is directional. Surfaces can give either specular or diffuse reflection. **Specular** surfaces described as mirror like, or glossy will have nearly zero reflectance at all angles except the appropriate reflected angle(angle of reflection equals to angle of incidence). On the other hand **diffuse** surfaces such as matte paint or highly textured surfaces have a uniform reflectance, which means that radiation is reflected the same way or equally in all angles. Those surfaces are called Lambertian surfaces.[7]

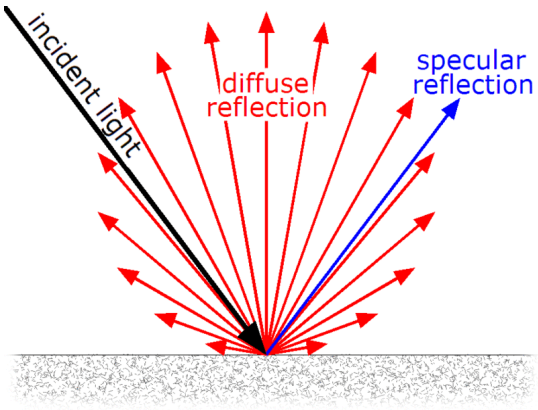

Fig.5: The way light is reflected in a diffuse and specular way.

It is important to note that while most real objects have a mixture of diffuse and specular reflective properties for the purposes of this work we will focus on the diffuse ones. The reasoning behind it, is that in the case of specular reflection the interaction between light and matter is not revealing of the surface's chromatic appearance since the reflected light has the spectral signature of the illumination source.

Color Stimulus

Now that we have defined the main components in the process of color perception we are in position to describe how color stimulus is a combination of those aspects.

The color that we see, or record, is the product of the quantification of the above properties. That is expressed as: Stimulus equals the spectral power distribution of the light source, times the spectral reflectance of the colored object , times the spectral sensitivity of the observer(that being the cones in the human eye, or the properties of a digital sensor or those of a photographic film)

For a Lambertian surface and following the model described above, the formulation of color response is expressed mathematically as:

$$c_i = \int_{\lambda e \Omega} I(\lambda) \cdot R(\lambda) \cdot S_k(\lambda)\, d\lambda \qquad (1)$$

where $\mathrm{I}(\lambda)$the scene illumination $\cdot\, \mathrm{R}(\lambda)$ the specral reflectance content

and $\mathrm{S_k}(\lambda)$ the cone sensitivity

with $\mathrm{k}\ \varepsilon\ \{\mathrm{S,M,L}\}$ for the tristimulus values model-that is a trichromatic observer.[3] Ω denotes the human eye visible spectrum range .

One can consider that the signals described above can be perceived as discrete given sufficient sampling rate, and so Eq(1) can be written as a summation of products.

$$c_i = \sum_{j=0}^{N-1} I(\lambda) \cdot R(\lambda) \cdot S_k(\lambda)\, \Delta\lambda \qquad (2)$$

the sampled wavelengths $\{\lambda\}_{j=0}^{N-1}$ are thought to be uniformly spaced over Ω.

Thus **c** can be arranged as 3 x1 matrix vector known as a tristimulus vector, that when associated with a standard condition can uniquely specify a color.

This connection leads us to the CIE CMF's (color matching functions) and the CIE standard color spaces.

Color Spaces

CIE XYZ Color Space

One of the most widely used standard basic color space is the CIE* 1931 XYZ color space(based on the works of Smith and Guild 1931) which covers all color sensations that an average person(observer) can experience. It is built on, and mathematically derived from the CIE RGB color space(work of Wright 1929) with modified primaries in order to avoid negative stimulus values. The color matching functions of the CIE RGB color space $\bar{r}(\lambda)$, $\bar{g}(\lambda)$, $\bar{b}(\lambda)$ are the result of experiments where each of the monochromatic test primaries was matched by normal observers through the adjustment of three RRG primaries combinations. This tackled the difficult problem of directly measuring the estimation of LMS cone sensitivity. Continuing, the CMF's of CIE 1931 XYZ are set by defining Y primary as the luminosity efficiency curve(which as can be seen is roughly analogous to the sensitivity of the M cones), Z as blue stimulation (almost equal to the S cone response) and X as a linear combination of cone responses explicitly chosen to be nonnegative.

Following our approach to the mathematic expression of LMS tristimulus, XYZ tristimulus in terms of standard observer are given by:

$$X = \frac{1}{N}\int_{\lambda e \Omega} I(\lambda)\cdot R(\lambda)\cdot \bar{x}(\lambda)\, d\lambda$$
$$Y = \frac{1}{N}\int_{\lambda e \Omega} I(\lambda)\cdot R(\lambda)\cdot \bar{y}(\lambda)\, d\lambda$$
$$Z = \frac{1}{N}\int_{\lambda e \Omega} I(\lambda)\cdot R(\lambda)\cdot \bar{z}(\lambda)\, d\lambda$$

$$N = \int_{\lambda e \Omega} I(\lambda)\cdot \bar{y}(\lambda)\, d\lambda \qquad (3)$$

where $\bar{x}, \bar{y}, \bar{z}$ the CIE standard observer color matching functions.

The XYZ color space serves as a reference standard space against which most other color spaces are defined, usually at an absolute Cartesian relation (main primaries, white and black point)

CIE color matching functions , standard observers

The distribution of photoreceptive cones in the human eye causes differences in the perception of color depending on the viewing angle of a visualized object.

This can be clearly explained by Figure 3.a, where one can notice the relevant absence of the S type cones in the centre of the fovea, and their abundance in the surrounding areas.

It has been determined that color perception differs when the viewing angle is 2 degrees or less, than when it is between 4 to 10 degrees as a result of incidence of photons on different parts of the retinal fovea.CIE 1931 standard colorimetric observer is thus used to represent the mean chromatic response of the human eye at a viewing angle of 2° degrees or under.In 1964 CIE published a new set of color matching functions in order to accommodate the need of a standard observer for a viewing field angle of 4° degrees or more. The empirical measurements were the result of experiments held for a 10° degree angle and thus the CIE'64 functions are usually referred to as the 10° degree standard observer.

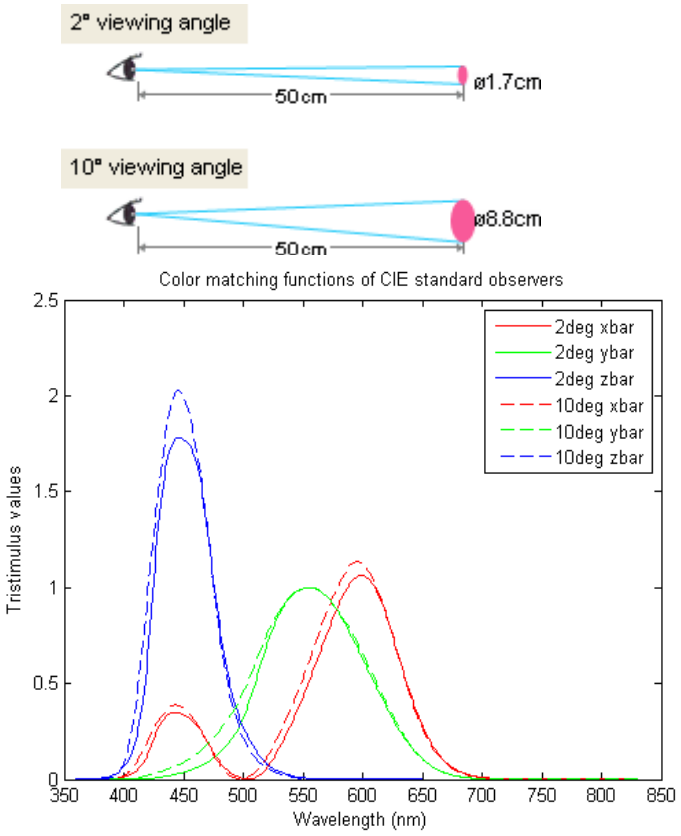

Fig.6:(a)representation of the two angles of view for the CIE CMFs. From Konicaminolta.com(b)the tristimulus values of the standard observers as a function of wavelength

xyY color Space

Since we defined Y as luminance, for any given constant Y value the two-dimensional XZ plane contains all possible chromaticities for that luminance.

The chromaticity parameters x , y are two of the three normalized values , functions of the tristimulus X Y Z .

$$x = \frac{X}{X+Y+Z}$$

$$y = \frac{Y}{X+Y+Z}$$

$$z = \frac{Z}{X+Y+Z} = 1 - x - y \tag{4}$$

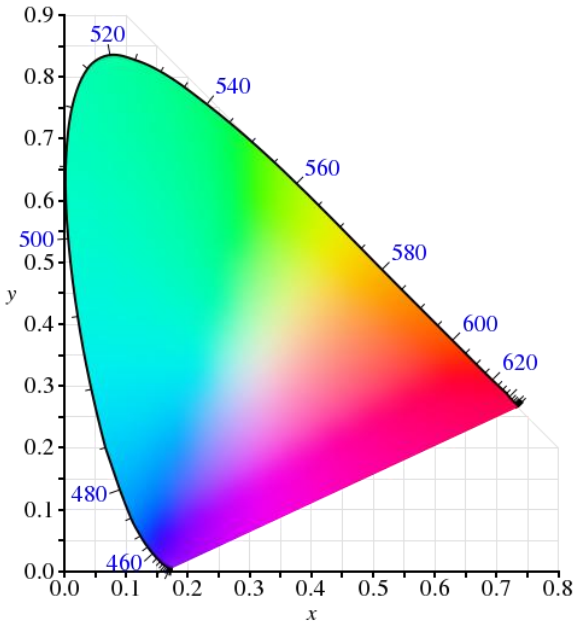

Fig 7.: The xyY chromaticity diagram for Y=1(max luminance).

The diagram represents all of the chromaticities visible to the average person. These are shown in color and this region is called the gamut of human vision(horseshoe-shaped figure). The curved edge of the gamut is called the spectral locus and corresponds to monochromatic -spectral- light (each point representing a pure hue of a single wavelength), with wavelengths listed in nanometers. It illustrates a very interesting quality of the CIE1931 color space. That is the existence of mathematically possible colors that are not visible to the human eye("imaginary" colors).

Working Color Spaces

SRGB

SRGB is the three dimensional color space we transformed our spectrally produced colors into, in order to be able to display them on a screen. It is widely accepted and used since its primaries and its gamma curve(as a transfer function) can be displayed properly on most computer screens. The gamut of chromaticities that can be represented in sRGB is the color triangle defined by its three primaries(the colors where one of the three channels is nonzero and the other two are zero). As with all RGB color spaces, for non-negative values of R, G, and B it is not possible to represent colors outside this triangle. The sRGB has a non linear step that is expressed with an approximate gamma value of 2.2.

CIE LAB

The CIE Lab color space is an immediate derivative of the XYZ color space. The intent of its creation was a color space that was more perceptually uniform to the human eye. Its components are **L** (lightness) and the two color components **a**, and **b**. As depicted in the figure below, the **a** axis is associated with red and green components; while the **b** axis is associated with the yellow and blue components. Note that in CIE Lab, a color cannot be composed by both yellow and blue, nor can be made of green and red. This model is called **a color opponent process**. L*, represents the darkest black at L* = 0, and the brightest white at L* = 100. The color channels, a* and b*, will represent true neutral gray values at a* = 0 and b* = 0.

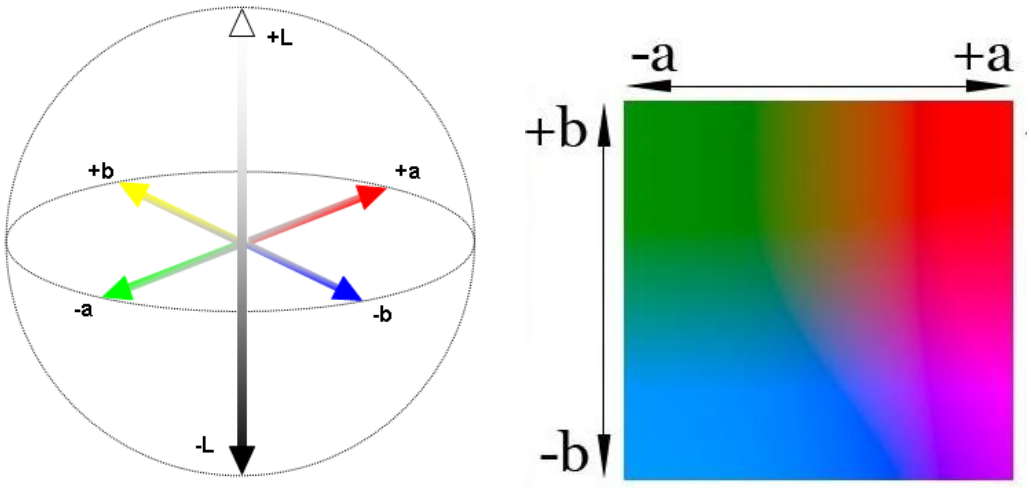

Fig.8: a)A three dimensional representation of the LAB color space. b) a cross section of the LAB space for lightness value of 50%

Metamerism

It is clear that the transformation from spectra to color is not lossless, as information has been lost during the mathematical projection/integration from high dimensional space -spectral power distribution- signal to a much lower dimensional tristimulus. One of the most important issues that occur is metamerism. Metamerism is defined as the matching of the color of objects as humans perceive them without matching their spectral power distribution.

The types of metamerism

- Illuminant metameric failure. Material samples match in color under a specific illuminant but not under another. Our work will focus on understanding and trying to tackle this type of metamerism.
- Geometric metameric failure. The metameric match or mismatch depends on the scene geometry and the incidence and reflectance angles. It is not concerning in our work, since we supposed that all reflective surfaces will act as Lambertian ones and thus diffusely reflect light equally to every direction.
- Observer metameric failure. The metameric match or mismatch depends on physiology of the observers vision system, e.g. differences in the eyes of different people. The use of a standard colorimetric observer more or less solves this problem since it assumes a "mean" representation of color matching functions for the average person and takes these deviations into consideration.
- Field-size metameric failure. Is the result of different analogies of cones in the centre or periphery of the retina. Accounted for, with the use of different colorimetric standard observers, used for different viewing angles. Does not have a significant impact on the simple tristimulus model.

Degree of metamerism: Difference in the spectral composition of two metamers(a metameric pair). A great degree usually means "probable failure".

In order to measure and quantify metamerism two kind of metrics are used.

Color rendering index(CRI): CRI is a linear function of the Euclidean distance between a reference and a test sample spectral vector.

Metamerism Index(MI): It is the mean chromatic distance of the metameric chromaticities when those are represented in the L*a*b* color space.

$$MI = \sqrt{(\Delta L_{n1} - \Delta L_{n2})^2 + (\Delta a_{n1} - \Delta a_{n2})^2 - (\Delta b_{n1} - \Delta b_{n2})^2}$$

where n1 is the first illuminant, n2 the second illuminant and

$$\Delta = Value_{sample} - Value_{reference}$$

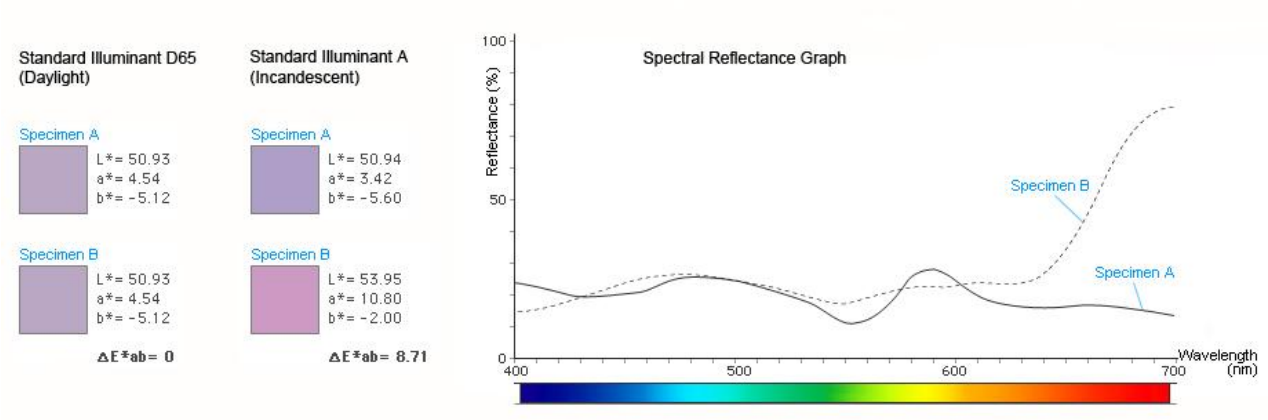

Fig.9: Example of how a pair of two metameric specimens with different spectral reflectance matches under a specific Illuminant(Standard D65) while they mismatch under another(Standard A).From Konicaminolta.com

Metamerism is an inherent problem that the additive tristimulus models we use to reproduce color have, since a given set of tristimulus values can be matched to practically infinite spectral curves.

A colorimetric approach is thus insufficient and the need for a spectral approach is clear.

Metamerism in nature

In natural scenes illuminated by daylight , the relative frequency of metameric surface pairs as a proportion to the total of pairs of surfaces in the scene is very low. Still, given surface pairs that were indistinguishable under one of those illuminants, the conditional relative frequency of metamerism was much higher [10]. The effect of the problem becomes greater with the increase of variance of incident light, and the addition of human made materials and colorants.

Spectroscopy

Spectroscopy began as the study of the interaction between matter and radiation as a function of wavelength. It originally referred to the use of visible light dispersed according to its wavelength, e.g. by an optic prism. The concept was later expanded in order to include any measurement of a physical quantity as a function of wavelength or frequency. An extension of the definition added energy as a variable after the realization of the Planck constant and its relationship with energy **E=h v**(v denotes frequency).

Spectrophotometry is the spectroscopic technique used to measure the reflection or transmition properties of a material. In chemistry it is used to assess the concentration or amount of a given substance in a solution. The instruments used to perform spectrometric measurements are spectrometers or spectrographs.

Spectroscopy/spectrometry has great application and it is an invaluable tool in the fields of astronomy and remote sensing. Most scientific telescopes are equipped with spectrometers, in order to measure the chemical composition and physical properties of celestial objects or to measure stellar velocities from the Doppler shift of their spectral lines.

Spectral Imaging

Spectral imaging(also referred as imaging spectroscopy or chemical imaging) is the application of spectroscopy to every pixel in a spatial(two dimensional) image.

The output of a spectral imaging system is a *spectral cube* or *lambda stack*. It contains spectral data(radiance) in a three dimensional notation (x, y, λ) where x, y are the spatial coordinates and λλ is wavelength.

It allows us to detect the nature of depicted surfaces or materials by being able to analyze the spectral data(reflective, transitive ,or emitted) of every pixel in an image and thus detect the materials present in the scene via their spectral identity(as noted before dependent on a materials chemical and physical properties).

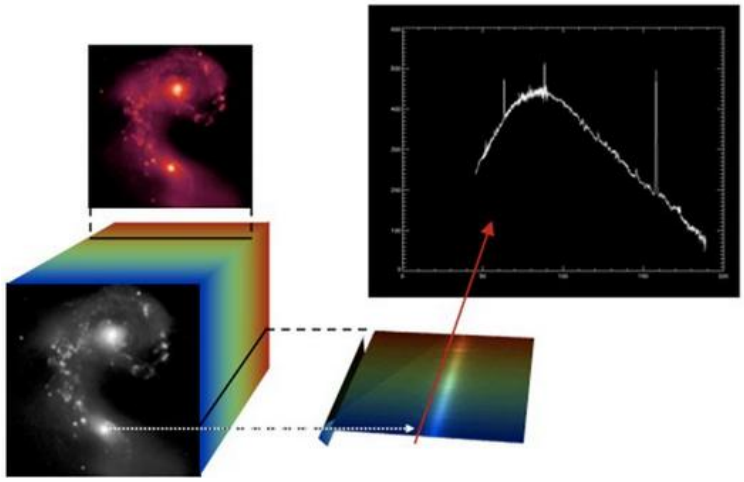

Fig.10:The structure of a spectral cube. For every pixel in the spatial image we store its spectral information.

The most basic parameters used to compare spectral imaging systems are the spectral range(the part or portion of electromagnetic spectrum they cover) the spatial resolution(amounts and ratio of image pixels) and spectral resolution(wavelength intervals of the lambda dimension),number, width and contiguousness of bands used.

Based on the above criteria(usually on an arbitrary number of bands) or on the type of measurement we can distinct spectral imaging into two main categories. Multispectral and Hyperspectral Imaging.

Multispectral imaging deals with several images at discrete and somewhat narrow bands. Being "discrete and somewhat narrow" is what distinguishes multispectral in the visible from color photography. A multispectral sensor may have many bands covering the spectrum from the visible to the longwave infrared. Multispectral images do not produce the "spectrum" of an object. For that purpose a method known as Spectral Prediction or Spectral Estimation is employed.

Hyperspectral deals with imaging narrow spectral bands over a continuous spectral range, and produce the spectra of all pixels in the scene. So a sensor with only 20 bands can also be hyperspectral when it covers the range from 500 to 700nm with 20 bands each 10nm wide. (While a sensor with 20 discrete bands covering the VIS, NIR, SWIR, MWIR, and LWIR would be considered multispectral.). As a relatively new analytical technique, the full potential of hyperspectral imaging has not yet been realized.

In case the spectral data is available in higher integral (e.g. 20nm) or its range is smaller than indicated (e.g. 420 – 700nm), interpolation or extrapolation of the data is suggested to meet the application requirements.

We can additionally classify spectral imaging systems based on the method used to acquire the spectral cube.

Instantaneous, or single exposure or snapshot systems are as the names describe able to obtain the spectral data during a single integration time of the detector array so that no spatial scanning is involved.Such Systems are advantageous in that they allow for a large increase in light collection efficiency(optical throughput) and a significant increase in the Signal to Noise Ratio of the measurements. Those characteristics increase geometrically with the corresponding increase in measurement dimensionality(dramatic for larger data cubes).Other important advantages include the lack of scanning artifacts and the increased robustness or compactness due to the lack of moving components , as well as the faster collection and process of data allowing more time to be spent on analysis.However, computational effort and manufacturing costs are high.A Bayer-Filtered digital camera (a familiar imaging system to most) can be considered a very simple form of Snapshot Spectral Imager since it captures the I(x, y, λλ) data-cube in a single exposure (where λλ=3 for Red, Green, Blue Bayer filter).

Scanning systems are the typical form of existing Spectral Imagers primarily used before the technological breakthroughs that made snapshot systems more accurate and less complex to manufacture. Those can be categorized based on the prioritization of the spectral cube dimensions and the stack completion sequence.

- Point-scanning (whiskbroom) spectrometer: Recover spectrum for a point location: I(x_i, y_j ,λ)
- Line-scanning (pushbroom) spectrometer: Recover spectra for one spatial dimension: I(x , y_i ,λ)
- Wavelength-scanning spectrometer: Recover two spatial dimensions for an integrated wavelength range: I(x, y,λ_κ).

All scanning spectral imagers scan in time to assemble the 3D cube of information from multiple 2D projections or slices.

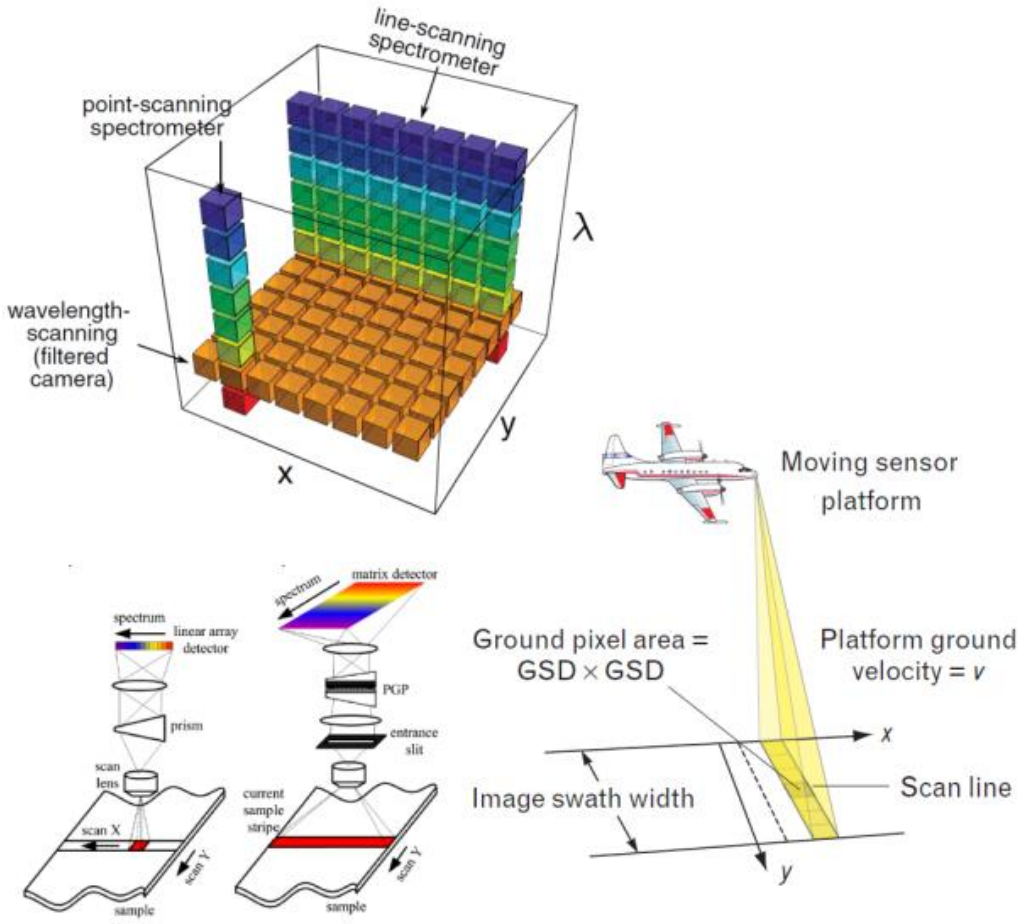

Fig.11: Spectral Scanning Methods and how they are implemented and used in airborne and remote sensing applications.

Hybrid scanning systems described as *spatiospectral scanning* exist and are uniting some advantages of spatial and spectral scanning, thus alleviating some of their disadvantages. They are based on the principle of placing a camera at some non-zero distance behind a basic slit spectroscope or by placing a dispersive element before a spatial scanning system[11][12]. Such systems require robust algorithms for image and data registration

Spectral Imaging Applications

Spectral Imaging Systems are used in a wide area of Applications.

In the field of *Agriculture* in order to solve problems in Farm mapping, Biomass mapping, Precision Farming, Plant disease detection, Crops and parasitic weeds detection, Tree growth rate evaluation and food inspection.

In *Environmental Studies* for : Deepwater Horizon oil spills, Sorting of plastics, Bathymetry, Hydrology, Waste sorting, Forest study and Forest fire management.

In the *Medical Field* for: Fever detection, Cancer detection, Cellular spectral imaging, Assessing burn injuries and various other Medical diagnostics, such as Skin diseases (psoriasis, neurodermitis, etc.) Cosmetics (precise color measurements, etc.)Blood measurements(oxygenation, etc.)

In *Defense and Security* in order to: Detect narcotics, detect Land mines, detect Perimeter breaching, Night vision and security monitoring, Search and rescue missions, Fire fighting, Maritime Applications such as such as drug trafficking, smuggling, human trafficking and illegal border crossings interception.

Geology applications that cover: Imaging lake sediments, Exploration of Archean gold, Hyperspectral core imaging, NIR core imaging and mineral classification, High speed drill core analysis.

In *Arts and Color Sciences* as well as History researches: Color pigment detection, Color variation recognition, Color quality control, Art imaging and under-drawing inspections, Ancient scrolls and texts research, Document legibility, Artwork diagnostics.

Color Reproduction using a Multispectral System

As we have stated before a three dimensional basis is a somewhat poor choice to express the illuminant and reflectances of a scene and be able to extract their effect on color.In the works of Parkkinen and Jaaskelainen on munsell colors, it is stated that a 6 to 8 dimensional basis is considered necessary [13][14] .

Our work focuses on color reproduction in a similar way to what is described as Garida Six Unmixed Bands Multispectral Imaging System in the work of D. Iliou.[9]. It is a novel snapshot system developed in the Electronics Laboratory allowing both for a fast approach and quick reproduction with satisfying results, as well as a full spectrum analytic approach, yielding quality color results directly connected to the spectral characteristics of the captured scene.

This method deploys two tri band pass optical filters at complementary wavelength ranges , capturing six spectral samples per pixel in the visible range as well as Infra red information the usefulness of which will be discussed further in a next section.

Capturing an image with each of those two filters allows us to form a x,y,6 dimensional spectral cube where x, y are the spatial resolution coordinates. A maximally reflective (completely white) surface is also captured to allow us to detect the illumination. After the color channels are unmixed and the illumination detected or estimated we solve our spectral data for spectral reflectance. For a fast approach, we can use our 6 discrete samples or combine them with interpolated interim values, but if we want a full spectral analysis we must first estimate the continuous full spectrum. We can then proceed to reproduce the color based on a different illumination or observer using the CIE XYZ tristimulus functions. Finally we can transform the color vectors from our reference color space to any working color space, suitable for our application (sRGB for displaying image on an computer screen CMYK for printing etc).The whole procedure is explained in greater detail in the following chapters. Below we present the system's Functional Diagram.

True Color Image Formation Flowchart

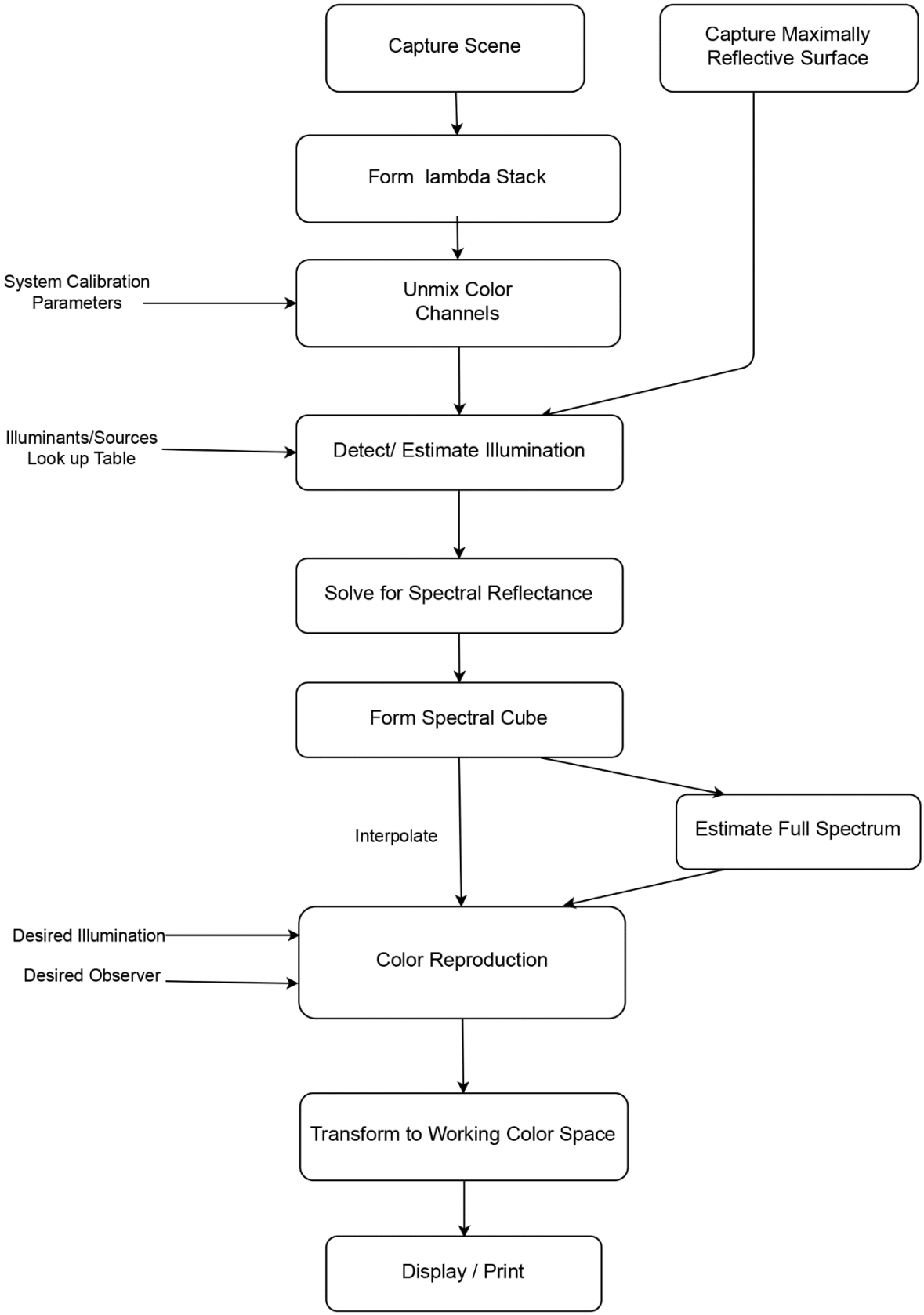

Methodology

How to measure Spectral Reflectance

In order to obtain the reflectances of the colorimetric chart patches one has to perform a Spectral Reflectance measurement of a single point, using a spectrometer.

The spectrometer that was used is by default set in Scope Mode. Scope data is the raw signal of the spectrometer, greatly influenced by its "**instrument response function**", or IRF. The IRF refers to how much the spectrometer responds to light across its wavelength range, a response that is not uniform. A spectrometer will produce a different response (here defined as the number of Scope-mode counts produced for a fixed number of photons) at every pixel of its array. The IRF is non-uniform because of the aggregated effects of optical inefficiencies in the light path. These include:

•Attenuation of light in the fiber optic cable
•Absorbance of light by the mirrors (which varies with wavelength)
•Grating efficiency
•Detector response (the CCD is more sensitive to some wavelengths than others)
The IRF for each spectrometer is unique, and cannot really be measured, just radiometrically approached.[15]

To *solve* the Scope mode data for Spectral Reflectance one needs only to divide with a *Reference measurement* of the light source or a maximally reflective surface. The white patch of the colorimetric chart can be used as such a surface. The resulting signal has been 'cleared' from the IRF since its contribution would be present in both the numerator and denominator of the fraction of this division. Hence spectral reflectance measurements are in a way device independent.

The same principle applies to spectral imaging as well, where one has to divide the intensity value of every pixel by the intensity value of the light source at that specific spectral band. In that way one can solve for spectral Reflectance of every single pixel and normalize the values at the 0-100 range as well.

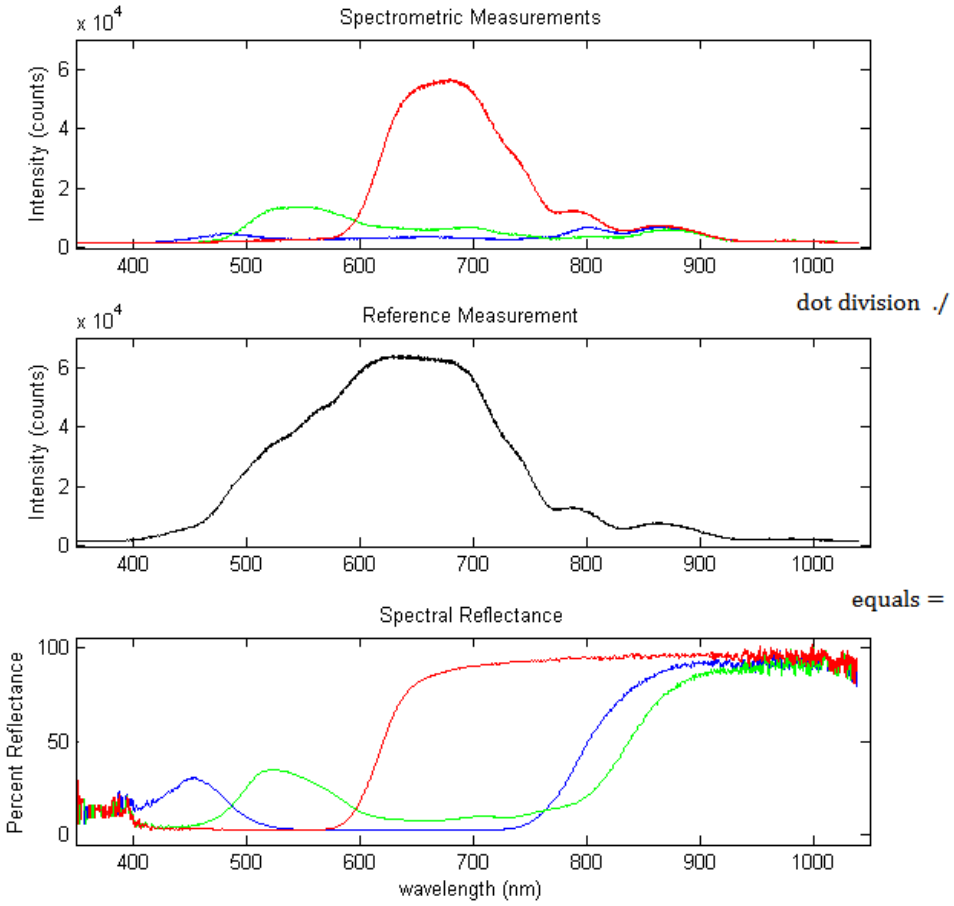

Fig.12: Spectrometric values of CC140 patches 4E,4F,4G. The initial Data is hugely distorted by the instruments response function. By dividing the value at each wavelength with the corresponding one from a reference measurement(in this case the maximally reflective white patch of the CC) we can obtain the unaffected Spectral Reflectance of the measured patches. Spectral Reflectance measurements should yield the same result regardless of the employed light source, given it is broadband enough to cover the range of interest. Below we see the spectral reflectance of those three color patches over the visible range.

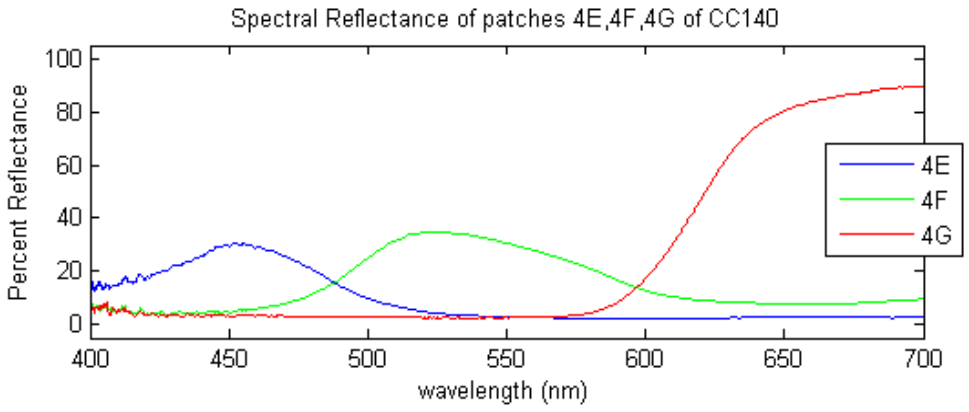

How to measure a Light source's Relative Irradiance

In order to be able to detect a light source present in a scene and reproduce the color of the scene under any illumination we first needed to measure a variety of available light sources both scientific as well as common ones used in daily life.

Irradiance measurements are influenced by diffraction grating spectral efficiency, used sensor spectral sensitivity and used optics spectral transmission. The two common corrections are Relative Irradiance and Absolute Irradiance calculations.

For Relative Irradiance a lamp with a known color temperature (but not necessarily known power output) is used to correct just the shape of the spectrum but not the magnitude (thus not absolutely but in a "relative" manner). Relative Irradiance allows the user to determine whether there is more light at one wavelength than another (which cannot be determined from Scope mode due to the IRF), though it does not provide any information on how much power there is in absolute terms.[16] *Such measurement is used for a qualitative comparison of different illumination sources and the expression of rules for the detection of a singular unknown source from a list of known light type spectra*.

The calculation for Relative Irradiance is as follows:

$$I_{L,T} = N * B_{L,T} * (S_L - D_l)/(R_L - D_L)$$

where:
$I_{L,T}$ is the relative irradiance at wavelength L and color temperature T Kelvins
N is a normalizing term to bound $I_{L,T}$ into the range *0-100*
S_L is the sample spectrum at wavelength *L*
D_L is the dark spectrum at wavelength *L*
R_L is the reference spectrum at wavelength *L*
$B_{L,T}$is the emission of a blackbody radiator at wavelength L and color temperature T in Kelvins.

We compute $B_{L,T}$ from Planck's law*:*

$B_{L,T}$=2*h*c^2 / (L^5 *($e^{(h*c / L*k*T)}$ -1))

where:
L is the wavelength in meters
T is the temperature of the blackbody in Kelvins
h is Planck's constant (≈6.626 * 10-34 J*s)
k is Boltzmann's constant (≈ 1.38 * 10-23 J/K)
c is the speed of light (≈ 3 * 108 m/s)
e is the base of the natural logarithm (≈ 2.718)

The computation of N requires the wavelength at which the maximum output for a blackbody of a given temperature occurs. This is done using the Wein displacement law (shown here, with an approximate value):[15]

Lmax = 2898 / T

=> N = 100 / BLmax,T

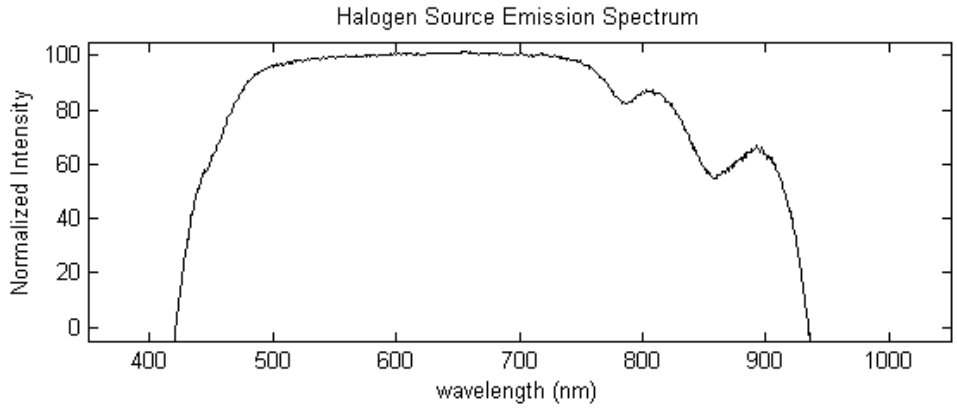

Fig.13: The resulting curve of a halogen source's relative irradiance measurement. Notice the difference with the Scope Mode intensity of the same source shown in Figure 20 b. Besides the IRF the signal has been cleared by the electric dark and electronic noise that initially affected it.

Formation of Spectral Color

Given a Spectral cube of greyscale images depicting the intensity of light, recorded by each pixel in the sensor of a camera, we recover the spectral reflectance of the objects appearing in the image. With the use of an illuminants curve and a color matching function we reproduce the color on a per pixel basis in the XYZ space.

After the whole procedure is repeated for the number of original pixels the Spectral Color or True Color image can be formed.

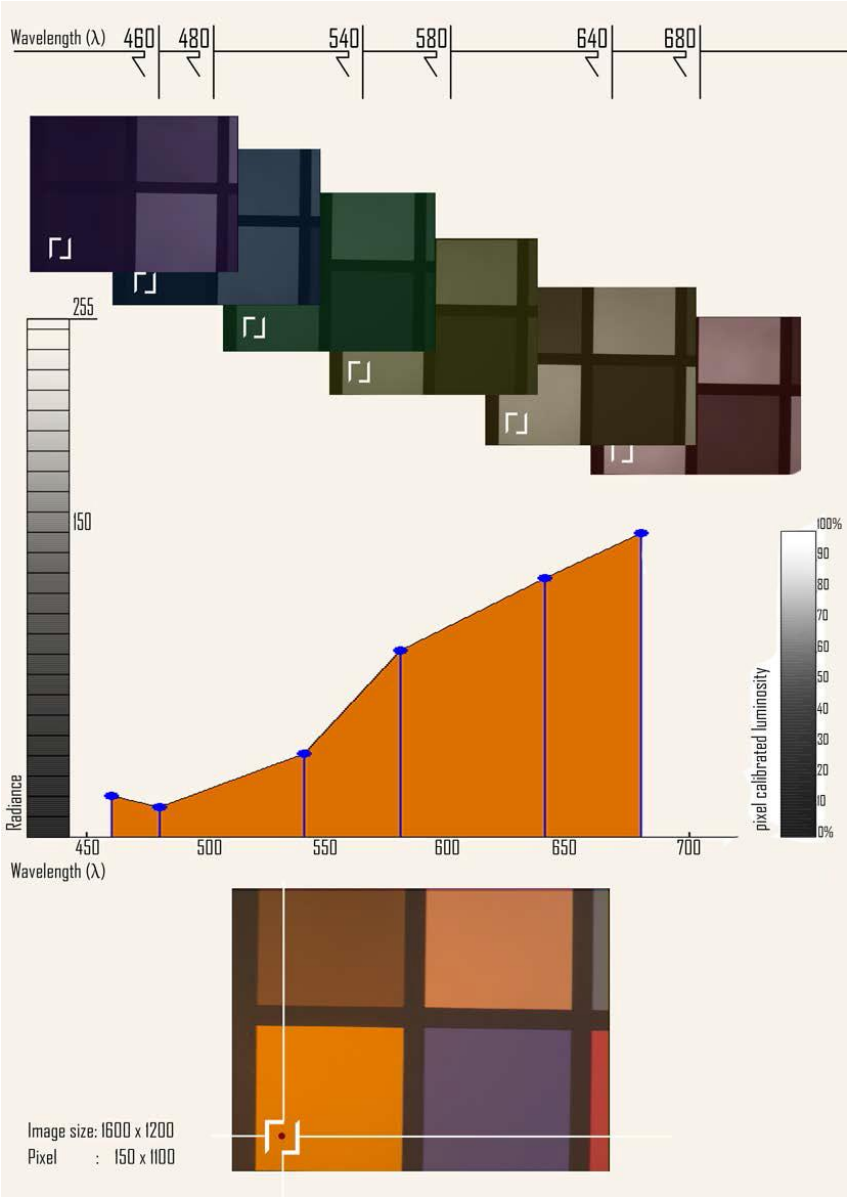

Fig.14: Color reproduction is a process repeated for every pixel in a Spectral Image. The spectral cube images here appear in color even though they are originally greyscale to emphasize their contribution in the final reproduction

Working Color Spaces and Conversions

SRGB

In the first section of this thesis we discussed about color reproduction in the CIE XYZ standard color space. While this give us a numerical representation of the produced color it does not suffice since we have to project this color to the user -just like every color in the image - through a medium in this case a computer screen. We also need to have a colorimetric basis on which we will calculate errors or deviations from an expected result. For these purposes, we converted our data into two of the most known working color spaces {sRGB} and {CIELAB}.

The RGB/XYZ transition Matrix

To convert from XYZ to RGB values(and vice versa) we use a transition matrix in terms of the RGB systems chromaticity coordinates (x_r, y_r, z_r), (x_g, y_g, z_g), and (x_b, y_b, z_b) and its reference white point coordinates (X_w, Y_w, Z_w),

$$\begin{bmatrix} X \\ Y \\ Z \end{bmatrix} = [M] \begin{bmatrix} R \\ G \\ B \end{bmatrix}$$

where

$$[\mathrm{M}] = \begin{bmatrix} S_r X_r & S_g X_g & S_b X_b \\ S_r Y_r & S_g Y_g & S_b Y_b \\ S_r Z_r & S_g Z_g & S_b Z_b \end{bmatrix}$$

with $\mathrm{X_r} = \frac{\mathrm{X_r}}{\mathrm{y_r}}$, $\mathrm{Y_r} = 1$, $\mathrm{Z_r} = \frac{(1-\mathrm{X_r}-\mathrm{Y_r})}{\mathrm{Y_r}}$,

and respectively for $(\mathrm{X_g}, \mathrm{Y_g}, \mathrm{Z_g})$, $(\mathrm{X_b}, \mathrm{Y_b}, \mathrm{Z_b})$

$$\begin{bmatrix} S_r \\ S_g \\ S_b \end{bmatrix} = \begin{bmatrix} X_r & X_g & X_b \\ Y_r & Y_g & Y_b \\ Z_r & Z_g & Z_b \end{bmatrix}^{-1} \begin{bmatrix} X_r \\ Y_g \\ Z_b \end{bmatrix}$$

so for the transition from our XYZ calculated values to RGB colors to display we required the inverse matrix $[T] = [M]^{-1}$.

Considering the sRGB specifications[17]and Standard Illuminant D65 as the reference white the matrix T is calculated as:

$$[T] = \begin{bmatrix} 3.2404542 & -1.5371385 & -0.4985314 \\ -0.9692660 & 1.8760108 & 0.0415560 \\ 0.0556434 & -0.2040259 & 1.0572252 \end{bmatrix}$$

The product of the XYZ matrix with T is a 3x1 matrix containing the linear RGB values. In order to get the proper sRGB values that reflect a typical monitor with a gamma of 2.2 we must act in a non-linear way(raising to a companding power).

The gamma corrected values are given by :

$$V = \begin{cases} 12.92v, & v \leq 0.0031308 \\ 1.055v^{1/2.4} - 0.055 & v > 0.031308 \end{cases}$$

where $V \in \{R_{srgb}, G_{srgb}, B_{srgb}\}$, $v \in \{R_{linear}, G_{linear}, B_{linear}\}$

CIE LAB

To convert from XYZ to LAB we use the following formulas.

$$L = 116f_y - 16$$

$$a = 500\left(f_x - f_y\right)$$

$$b = 200\left(f_y - f_z\right) \text{ where}$$

$$f_x = \begin{cases} \sqrt[3]{x_r}, & x_r > \varepsilon \\ \dfrac{\kappa x_r + 16}{116}, & x_r \leq \varepsilon \end{cases}$$

$$f_y = \begin{cases} \sqrt[3]{y_r}, & y_r > \varepsilon \\ \dfrac{\kappa y_r + 16}{116}, & y_r \leq \varepsilon \end{cases}$$

$$f_z = \begin{cases} \sqrt[3]{z_r}, & z_r > \varepsilon \\ \dfrac{\kappa z_r + 16}{116}, & z_r \leq \varepsilon \end{cases}$$

$$x_r = \frac{X}{X_r}, \qquad y_r = \frac{Y}{Y_r}, \qquad z_r = \frac{Z}{Z_r}$$

with constants $\boldsymbol{\varepsilon}$= $216/24389 (\approx 0.008856)$ and $\boldsymbol{\kappa}$=$24389/27 (\approx 903.3)$ [18].

The values Xr, Yr, Zr for the two most common reference illuminants can be found in Appendix[A1]

Delta E Color Difference Metric

The reason we transform our data from the XYZ tristumuli to LAB values is to take advantage of LAB's perceptual uniformity as well as its geometric orientation, that allows us to calculate $\boldsymbol{\Delta E^*_{ab}}$ a color difference formula that relates a measured color to a known set of CIELAB coordinates.

Delta E is defined as the Euclidean distance of the two colors, that is the length of the line segment connecting the two colors in terms of their Cartesian coordinates[19][20].

$$\Delta E^* ab = \sqrt[2]{(L_2^* - L_1^*)^2 + (a_2^* - a_1^*)^2 + (b_2^* - b_1^*)^2}$$

When the value of this metric is lower than 5, then high fidelity color reproduction can be performed with no significant perceptual differences from the origin.[9] Furthermore the value 2.3 is a threshold that corresponds to a **Just Noticeable Difference** (JND), which means that 2 colors with $\boldsymbol{\Delta E^*_{ab}}$ less than 2.3 will be indistinguishable from one another.

Chromatic Adaptation

Chromatic Adaptation is the ability of a vision system to maintain a relatively preserved appearance of colors by adjusting to changes in scene illumination. The human visual system is adaptive to such changes and thus is color constant. When the correction occurs in a camera it is referred to as white balance.

The three common algorithms for chromatic Adaptation are XYZ scaling, Von Kries transformation, and the Bradford transformation. The Bradford method is the newest of the three s, and is considered by most experts to be the best one [21] The Bradford transform is a linear transformation of a source color $(X_s Y_s Z_s)$ into a destination $(X_D Y_D Z_D)$ by a matrix $[M]$ depending on the source white point $(X_{WS} Y_{WS} Z_{WS})$ and the destination one $(X_{WD} Y_{WD} Z_{WD})$

There are three steps in the algorithm.

- Transform source XYZ into cone response domain(ρ,γ,β) with . $[M]$
- Scale the vector components by factors of the reference whites.
- Transform (ρ,γ,β) back to XYZ with the inverse matrix $[M]^{-1}$

- $$\begin{bmatrix} X_D \\ Y_D \\ Z_D \end{bmatrix} = [M] \begin{bmatrix} X_S \\ Y_S \\ Z_S \end{bmatrix}$$ where

$$[M] = [M_A]^{-1} \begin{bmatrix} \rho_D/\rho_S & 0 & 0 \\ 0 & \gamma_D/\gamma_S & 0 \\ 0 & 0 & \beta_D/\beta_S \end{bmatrix} [M_A]$$

- $$\begin{bmatrix} \rho_S \\ \rho_S \\ \rho_S \end{bmatrix} = [M_A] \begin{bmatrix} X_{WS} \\ Y_{WS} \\ Z_{WS} \end{bmatrix}, \qquad \begin{bmatrix} \rho_D \\ \rho_D \\ \rho_D \end{bmatrix} = [M_A] \begin{bmatrix} X_{WD} \\ Y_{WD} \\ Z_{WD} \end{bmatrix}$$

-
  - *The values of the transformation matrix can be found in Appendix[A1]*

Chromatic adaptation is used to determine the shifted position of the white point when calculating a color space transition matrix for a non native illuminant (e.g. the sRGB is defined relative to a D65 reference white while ICC profiles are defined relative to a D50 reference white).

Materials and Equipment

Colorimetric Charts

Macbeth Color Checker

The Macbeth Color Checker is a unique test pattern scientifically designed to help determine the true color balance or optical density of any color rendition system. It is an industry standard that provides a non-subjective comparison with a test pattern of 24 scientifically prepared colored squares. Each color square represents a natural object—human skin, foliage, blue sky, etc providing a qualitative reference to quantifiable values. Each color will reflect light in the same way in all parts of the visible spectrum, thus maintaining color consistency over different illumination angles. It is widely used in the field of Spectral Imaging [14]. In our study, we use Macbeth Color Checker mostly as a priori samples

.

Fig15 Gretag Macbeth Color Rendition Chart. From http://xritephoto.com/documents/literature/en/ColorData-1p_EN.pdf

In the plots presented in this thesis Pad 1 is the upper left pad and we increase the number from left to right and by row. So the last pad is the Black on bottom right which is Pad 24.

Measured reflectance spectra are available on the Munsell Color Science Laboratory website taken from measurements published in Noboru Ohta (1997). "The Basis of Color Reproduction Engineering" (Japanese)

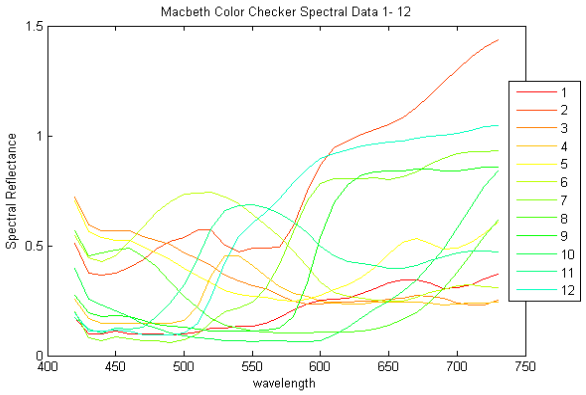

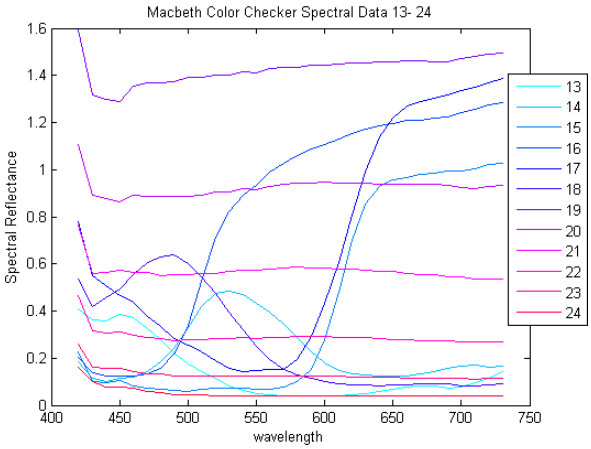

No.	Number	sRGB R	sRGB G	sRGB B	CIE L*a*b* L*	CIE L*a*b* a*	CIE L*a*b* b*	Munsell Notation Hue Value	Munsell Notation / Chroma
1.	dark skin	115	82	68	37.986	13.555	14.059	3 YR	3.7 / 3.2
2.	light skin	194	150	130	65.711	18.13	17.81	2.2 YR	6.47 / 4.1
3.	blue sky	98	122	157	49.927	-4.88	-21.925	4.3 PB	4.95 / 5.5
4.	foliage	87	108	67	43.139	-13.095	21.905	6.7 GY	4.2 / 4.1
5.	blue flower	133	128	177	55.112	8.844	-25.399	9.7 PB	5.47 / 6.7
6.	bluish green	103	189	170	70.719	-33.397	-0.199	2.5 BG	7 / 6
7.	orange	214	126	44	62.661	36.067	57.096	5 YR	6 / 11
8.	purplish blue	80	91	166	40.02	10.41	-45.964	7.5 PB	4 / 10.7
9.	moderate red	193	90	99	51.124	48.239	16.248	2.5 R	5 / 10
10.	purple	94	60	108	30.325	22.976	-21.587	5 P	3 / 7
11.	yellow green	157	188	64	72.532	-23.709	57.255	5 GY	7.1 / 9.1
12.	orange yellow	224	163	46	71.941	19.363	67.857	10 YR	7 / 10.5
13.	blue	56	61	150	28.778	14.179	-50.297	7.5 PB	2.9 / 12.7
14.	green	70	148	73	55.261	-38.342	31.37	0.25 G	5.4 / 8.65
15.	red	175	54	60	42.101	53.378	28.19	5 R	4 / 12
16.	yellow	231	199	31	81.733	4.039	79.819	5 Y	8 / 11.1
17.	magenta	187	86	149	51.935	49.986	-14.574	2.5 RP	5 / 12
18.	cyan	8	133	161	51.038	-28.631	-28.638	5 B	5 / 8
19.	white (.05*)	243	243	242	96.539	-0.425	1.186	N	9.5 /
20.	neutral 8 (.23*)	200	200	200	81.257	-0.638	-0.335	N	8 /
21.	neutral 6.5 (.44*)	160	160	160	66.766	-0.734	-0.504	N	6.5 /
22.	neutral 5 (.70*)	122	122	121	50.867	-0.153	-0.27	N	5 /
23.	neutral 3.5 (.1.05*)	85	85	85	35.656	-0.421	-1.231	N	3.5 /
24.	black (1.50*)	52	52	52	20.461	-0.079	-0.973	N	2 /

Cie L*a*b* values use Illuminant D50 2 degree observer sRGB values for Illuminate D65.

Fig16. a)ColorChecker Reflectance spectra divided into 2 plots (patches 1-12, and patches 13-24). b)ColoChecker Colorimetric Values per patch.

Xrite Color Checker SG 140

The Color Checker SG consists of 140 squares of paint applied to paper then mounted to a cardboard backing with a black frame around all the patches. There are 14 columns and 10 rows of patches. All the patches have a semi-gloss surface, which is represented by the SG in the name (Semi-Gloss). The outer patches are a pattern of white, gray and black patches.

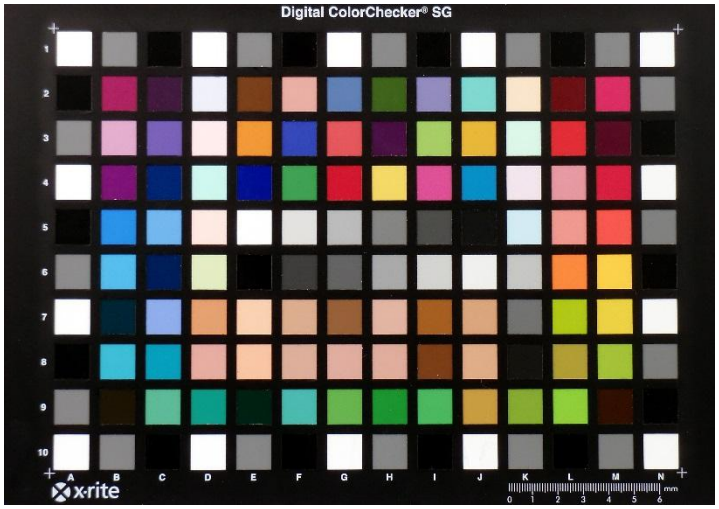

Fig.17 xrite Color Checker SG

There is a 6 x 4 pattern of patches which correspond in color to the original Color Checker. The spectra and colorimetric values of these patches are different from the original Color Checker so it cannot be used directly as a profiling substitute for a Color Checker without first making a new reference file by measuring this area with a spectrometer. This version of the colorimetric chart also contains a wide array of skin tone colors, more grayscale tones, and a subset of the Munsell representation space.

Hardware

Spectrometer: Ocean Optics USB 4000

This work required radiance and irradiance measures that are wavelength-specific by making separate serial measurements on a narrow range of wavelengths.

There are several types of spectrometers for these measurements. The most used type is the **diode-array** type because it is lightweight, fast, possesses no moving parts, and has low power requirements, so it can be used for 'on the field' applications. The device used is illustrated in Figure 14. The light signal from the sensor is brought into the instrument with a fiber optic cable and spread/split into a rainbow of colors with a diffraction grating. The dispersed light falls on an array of photodiodes, each of which responds only to the narrow range of wavelengths impinging on it. The diodes are connected to a charge-coupled device (CCD) that produces a voltage. Voltages from each diode are converted to digital counts and sent to a dedicated computer with spectrum analysis software. To compensate for the various types of noise several scans may be made and averaged in a matter of seconds.

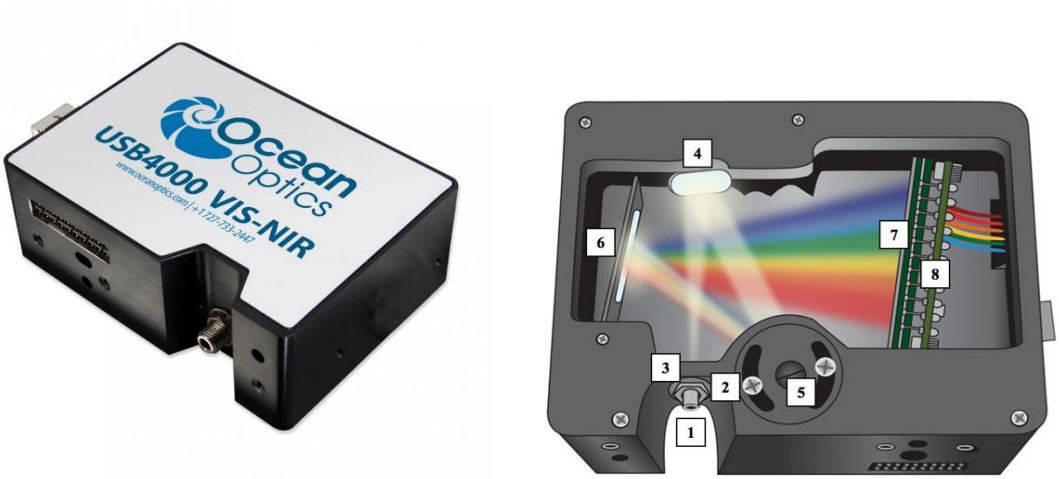

Fig 18. Diode-array spectroradiometer (Ocean Optics USB4000). Light enters the spectrometer from a fiber optic cable connected to a probe (1) controlled with an adjustable slit (2) and a filter restricts the wavelength range(3). The filtered light then encounters a collimator(4) that focuses the parallel ray beam on a diffraction grating (5). This grating scatters the different wavelengths, like a prism, onto a focusing mirror (6) that directs the light via a collector lens (7) onto the detector (8). The detector converts the optical signal to digital format.(*From Ocean Optics online manual*)

Spectrometer Specifications	USB4000
PHYSICAL	
Dimensions:	89.1 mm x 63.3 mm x 34.4 mm
Weight:	190 g
DETECTOR	
Detector:	Toshiba TCD1304AP (3648-element linear silicon CCD array)
Detector range:	200-1100 nm
Pixels:	3648 pixels
Pixel size:	8 µm x 200 µm
Pixel well depth:	100,000 electrons
SPECTROSCOPIC	
Optical resolution:	~0.1-10.0 nm FWHM (configuration dependent)
Signal-to-noise ratio:	300:1 (full signal)
A/D resolution:	16 bit
Dark noise:	50 RMS counts
Dynamic range:	3.4 x 10^6 (system); 1300:1 for a single acquisition
Integration time:	3.8 ms – 10 seconds
Stray light:	<0.05% at 600 nm; <0.10% at 435 nm
Corrected linearity:	>99%
ELECTRONICS	
Power consumption:	250 mA @ 5 VDC
Inputs/Outputs:	8 onboard digital user programmable GPIOS
Connector:	22-pin connector

Table of spectrometer specifications, as provided by the manufacturer.

ZWO ASI178MC color CMOS camera

For the needs of the 6 band Multispectral Imaging System we used a Back-illuminated CMOS Image Sensor.

ASI178MC has a 1/1.8″ and 6.4M pixels sensor IMX178 with SONY Starvis. It has low read noise(2.2 e),and high sensitivity features required for high precision spectral imaging.

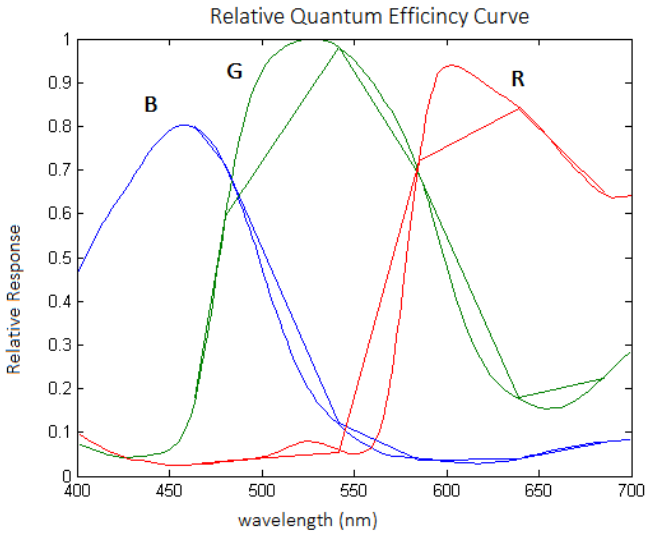

Fig.19: a)The ASI178MC camera that was used for the Multispectral Imaging method. b) The onboard CMOS Sensor's Quantum Efficiency curve as continuous signal all over the visible spectrum and as linear interpolated signal of 6 samples at the sampling wavelengths of the optical filters we used (explained below)

Optical Filters

Triple-Band Pass Filters

In order to obtain a meaningful 6 dimensional representation of a spatial image we needed to filter the light that passes to the CMOS sensor of the camera. That was achieved with the use of two complementary triple band pass filters since they allowed the acquisition of 3 narrow spectral bands each. The choice of the bands and thus were done based on the conclusions of D. Iliou in [9], and in such a way that fits the sensor's quantum efficiency curves. That is that every pair of bands is centered at a different pixel type of the sensor {R,G,B} considering the Bayer mossaic filter in from of the sensor.

The filters used were the Semrock 464/542/ 639 nm triple band pass filter, with corresponding band widths of 23nm,27nm and 42nm, Semrock 480/585/685 nm triple band pass filter, with corresponding band widths of 40nm,50nm and 50nm.The second filter also allows a wide band of IR spectra to pass through.It is considered an unwanted leak, and not described in the product's specifications but we can use it in a meaningful way for determining/estimating an unknown illuminating source.

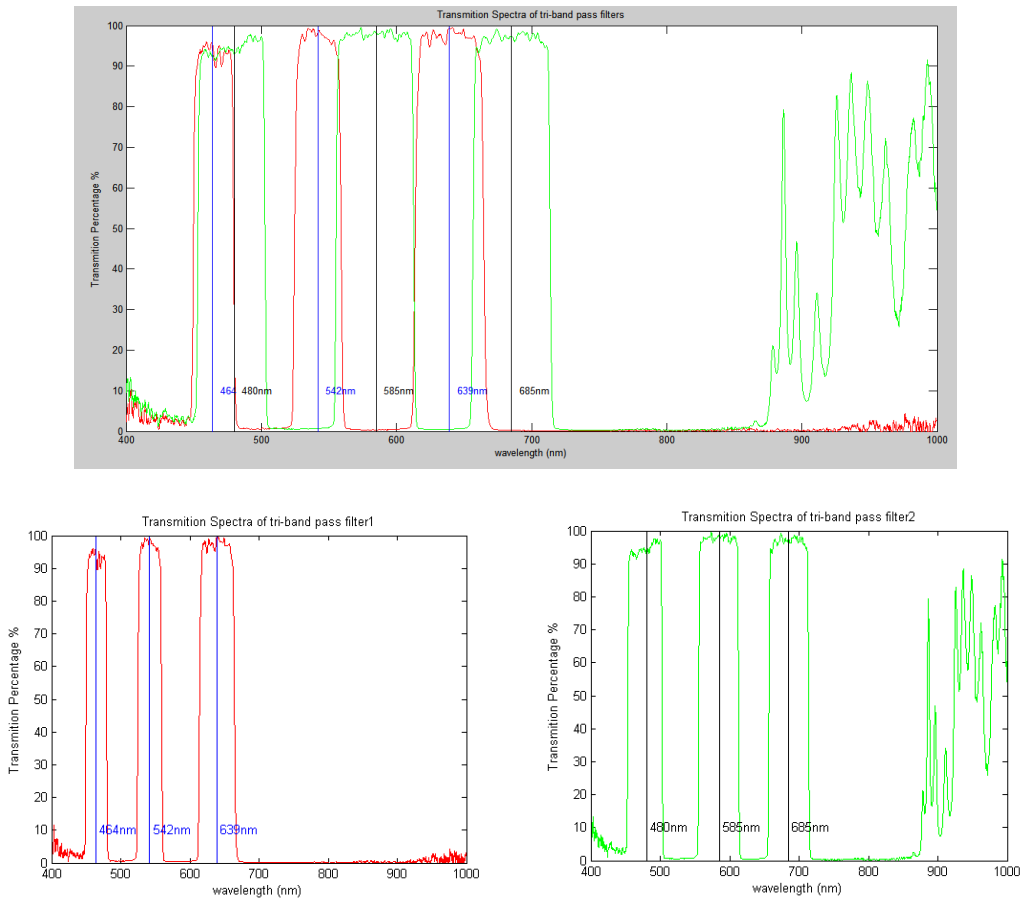

Fig.20: The complementary spectral bands and their centers with the use of two triple band pass optical filters

Fig.21: Optical Multiband filters of the same product line as the ones that were used.

IR cut, IR pass filters

It is known that you cannot produce quality color digital images without filtering out the Infra Red part of the rays incident to the CMOS sensor of a camera, since the pixels are sensitive to IR radiation and will store information that our eyes cannot see, ruining in that way the color fidelity of a picture. Thus in order to take IR free spectrum in our images we used an IR cut filter.

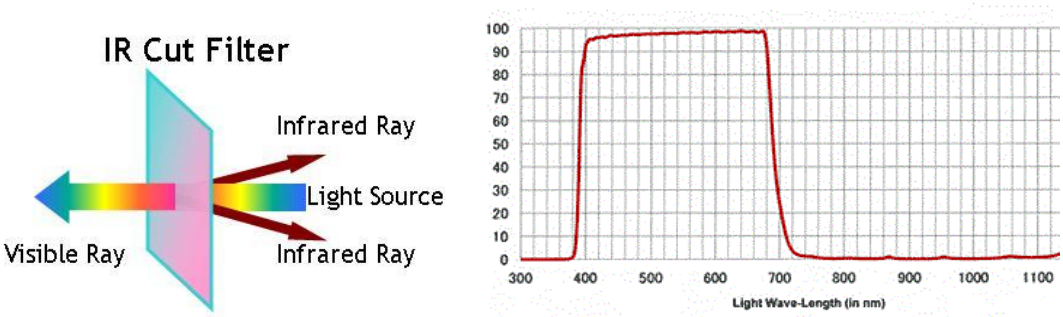

Fig.22. An IR cut filter and its spectral range. From toa-optical.com and tse-imaging.nl

During our research we studied the work of C.Fredembach and S. Susstrunk

in [27], that suggest the use of an IR image and each pixels information in order to help estimate the Illumination source of a scene. It is possible that with an extra image exposure and the use of an IR pass Visible cut filer we can acquire the IR information that one of the triple bandpass filters allows through and use it in such a way.

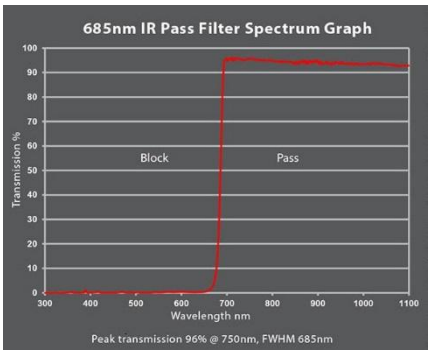

Fig.23. An IR pass Visible cut filter's spectral range. From altairastro.com

Software

For the purposes of this work three different software programs were used.

Spectra Suite: We used Spectra Suite the official Ocean Optics software for spectroscopic measurements that accompanies and is compatible with the spectrometer we used.

Spectra Suite allowed us to measure the relative irradiance of available light sources, measure the spectral reflectance of the colorimetric chart patches under different conditions, measure the transitivity of light through our optical filters as well as the sensor sensitivities. The methodology of said measurements is explained in detail in following sections.

MatLab: We used MatLab for all of our calculations and data plotting needs. MatLab allowed us to write scripts for Color Reproduction, Illumination extraction, Color space transition, Chromatic Adaptation, Measuring colorimetric differences, working with spectral data, organizing and plotting data in meaningful ways, as well as export and display our resulting images.

ImageJ: ImageJ is an open source image processing program designed for scientific multidimensional images. It allowed us to do analytic work on our images, and better manage our spectral cubes.
We used it to synthesize image stacks, divide images into their primary channels and also calculate image differences, image divisions, image histograms etc.

.

Experiment Description

Measuring Spectral Reflectance of the Color Checker SG140 under various illumination sources

To compare different sampling methods, with a varying number of spectral bands we needed to measure the spectral reflectances of the 140 patches of the colorimetric chart. We did that for multiple light sources to compare the results and conclude if our method is illumination independent.

For the experiment setup we used:

- Xrite ColorChecker SG140
- Ocean Optics USB4000 spectrometer
- Computer with Spectra Suite software

The light sources used were:

- Direct Sunlight at noon.
- White LED light source
- Thor Labs OSL1 light source
- Arkon Stay Cool Photographic Spotlights
- Typical domestic tungsten fillament Incandescent bulb.
- Typical Fluorescent Light tubes of two types.
- Typical domestic Halogen Light bulb.

To obtain the spectral reflectance two initial measurements are required and then 140 additional, one per patch. The first two measurements are the Reference measurement, and the Dark Reference. The reference measurement is performed on one of the maximally reflective patches, e.g. white patch 1a. with the lights on and is required to make the measurement IRF and illuminant independent as described in the method section of this thesis. The dark Reference is performed with the light source turned off, and is needed to measure the electric or other noise that is accumulated on the sensor's pixels.
The integration time is set depending on the light source's intensity and distance from the optic fiber to an amount that results in a 55k-60k counts on the curves maximum peak.

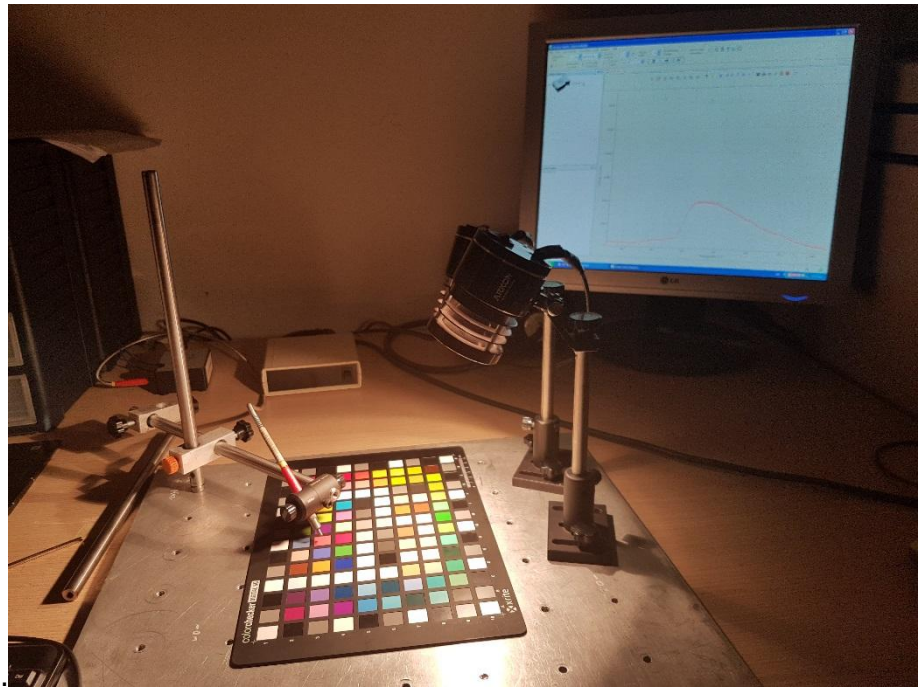

Fig.24 The experiment Setup. On the foreground the chart measured, optic fiber and the light source. On the background the spectrometer and a computer running the software.

Measuring the Spectral Power Distribution of various light sources.

For this part of the experiment a very similar setup was used. The light sources' relative irradiance , intensity values were measured by the spectrometer. In cases where a direct orientation of the optic fiber to the source was not easy or steady enough, a maximally reflective surface was again used since the reflected light will practically contain the light sources spectral information. For sources that follow the Planckian laws , a blackbody ratioator reference is required.

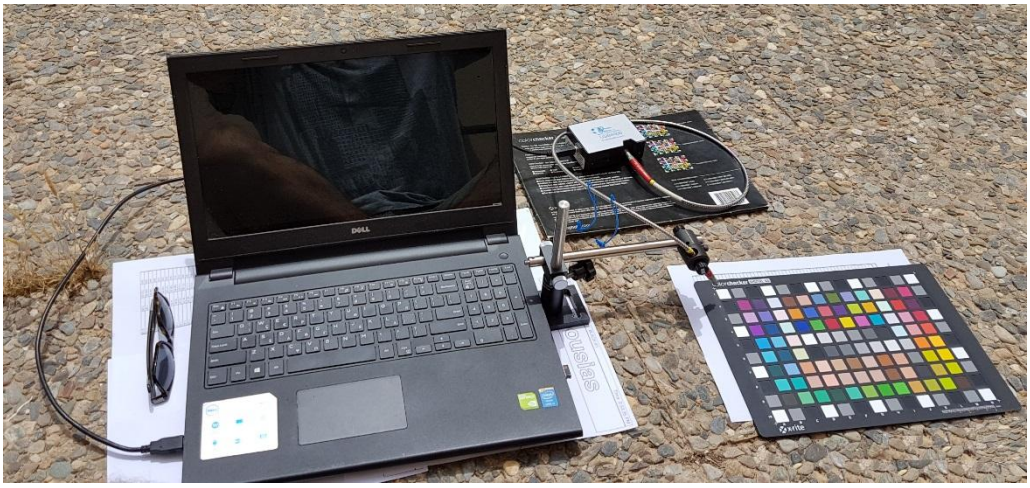

Six Narrow Band Snapshot Multispectral Imaging

Spectral Images were captured using a practical multispectral method that requires a bayer filtered CMOS camera and two triband pass filters. Images are captured in a single exposure and the spectral cube is formed after the images have been cleared from the pixel cross-talking.

For the setup we used:

- ZWO ASI178MC color CMOS camera
- Semrock 464/542/ 639 , Semrock 480/585/685 nm multiband pass filters
- 700nm+ IR cut filter.
- a broadband light source.
- computer to save the images and form the lambda stack.

Fig.25 The system setup. The multiband filters , and the IR cut filter are mounted onto the camera body. The object is set in place and the light source placed to point at it, from an angle that does not create specular reflections. The snapshot is captured and the image transferred to a computer for further analysis.

The camera setting o Gamma ,Gain, White balance and Exposure time found to work best for each filter are presented below

	464-542-639nm TBPF	480-585-685nm TBPF
Gain	41	41
Gamma	0	0
White Balance	Red: 39 Blue:99	Red:44 Blue:99
Exposure	285ms	235ms

Results and Discussion

Color Reproduction of Macbeth Color Checker

In order to evaluate our methods in reproducing color from spectral data for various illuminations , the Macbeth Color Checker was used.

The spectral data of the 24 patches were acquired from the book The Basis of Color Reproduction Engineering as mentioned in Figure 12 in the previous section.

Color was reproduced in the XYZ reference space and then transformed into linear RGB values, and after gamma correction into SRGB ones. The illuminants used were sunlight simulators , standard illuminant D50, standard illuminant D65 as well as the theoretical ideal equal energy illuminant E.

To calculate the accuracy in which color was reproduced, by comparing it to the expected values the colorimetric chart manufacturer provides, the colors were also transformed into the CIE LAB space, were the Delta E metric was calculated.

Two sampling rates were used to approximated the number of bands that could be used in a multispectral imaging system.

- 16 samples method (400nm to 700 nm with an interval step of 20 nm), which can be considered high spectral resolution
- 6 samples method(samples at 460,480,540,580,640,680 nm)

The results of those calculations can be seen in the images below. Each patch of the chart is represented by a single chromatic value and reconstructed in a 50 by 50 pixel .png format. The importance of proper gamma correction, in order to produce quality color is noticeable.

Color Reproduction using 16 samples (400:20:700nm)

Linear gamma SRGB colors **Gamma corrected SRGB colors**

under illuminant D50

under illuminant D65

under illuminant E

Figure 26 a: Reproduced Color of the Macbeth color checker under various illuminants.

Color Reproduction using 6 samples (460,480,540,580,640,680 nm)

Linear gamma SRGB colors **Gamma corrected SRGB colors**

under illuminant D50

under illuminant D65

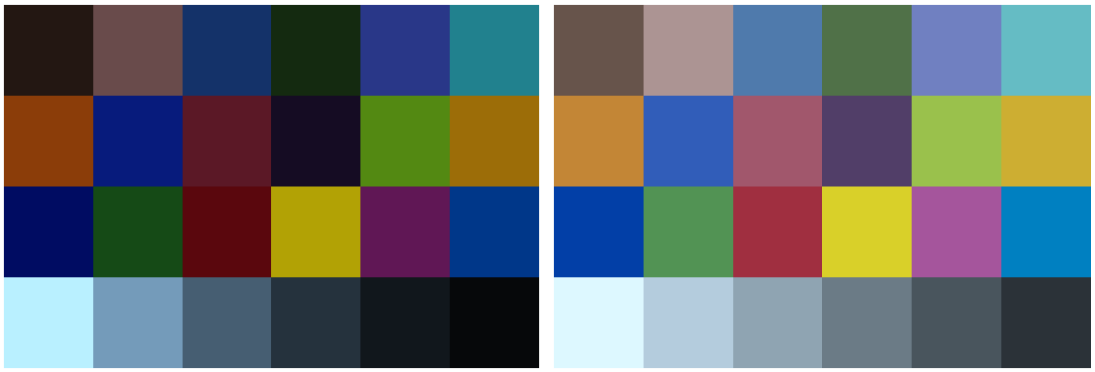

under illuminant E

Figure 26 b: Reproduced Color of the Macbeth color checker under various illuminants.

To realize the accuracy of those methods and the fidelity of the resulting color. The **ΔE*ab** metric between the equivalent CIELAB colors and the expected values of the chart[Figure 12] was measured.Since Lab values have D50 as the reference illuminant, the corresponding calculated colors were used.

ΔE*ab

Reproduction with 16 samples		Reproduction with 6 samples
0,860497666998057	Patch1	8,75578413887244
0,437366372608898	Patch2	17,3111210857583
1,46065708974134	Patch3	12,0243252478980
0,257279508821246	Patch4	7,99376393370622
0,676442473333060	Patch5	13,0416724234906
1,30412592926645	Patch6	17,2686655183363
1,10810115597646	Patch7	18,5723975740133
1,41776407865988	Patch8	11,2674740408795
0,851780546614331	Patch9	19,4003114410297
1,94610505500163	Patch10	5,28029398481797
1,02976232603738	Patch11	7,70034156962624
0,656537122176623	Patch12	18,2988769970889
1,77251230835023	Patch13	15,1269879369392
0,843856349100988	Patch14	7,83517221313628
1,92122877705420	Patch15	10,1372586978900
0,877250027730065	Patch16	15,0128011461305
0,495079718836852	Patch17	12,1062994461555
1,34374599418246	Patch18	24,6309766792398
1,08116763593756	Patch19	17,0088644464107
0,882178711216740	Patch20	14,6416572347903
1,04037327449482	Patch21	12,3577290344730
0,314399141166858	Patch22	10,5558003734100
0,713544902723660	Patch23	7,13844475024042
0,555699053065358	Patch24	4,99415668555317

max 1.9461		**max 24.6310**
min 0.2573		**min 4.9942**
mean 0.9936		**mean 12.8525**

Figure 27: Color Difference between Reproduced Macbeth patches and their expected values.

The results are satisfying both visually and numerically.

The value of Delta E is quite low in both cases especially considering the significant error margin, in the lower wavelength range of the spectral data (as shown in Figure 16).

In the case of color reproduction using 16 samples we measured the mean Delta E to be 0.99, an almost insignificant amount given the deviations in the charts real color data, spectrometric errors, as well as error introduced from color space transition and number rounding.

Notice how even the maximum value of DE is in that case 1.9461 which is lower than the threshold at which the human eye can detect chromatic differences(Just Noticeable Difference value of 2.3).

In the case of 6 samples the DE metric is higher almost by an order of magnitude..The effect of low sampling rate over the signal is quite clear, but it can be compensated with the use of spectral estimation.

Spectral Reflectances of Xrite Color Checker SG 140

The spectral reflectances of the SG 140 Color Checker were measured under different illuminants , with the method discussed in Section 2 of this thesisl.

Given that an illumination source is broadband enough to cover the whole visible range there should be little to no variance in the resulting data and thus to the resulting color under the same reproduction conditions.

We present the spectral reflectance data acquired using the Thor Labs OSL1 broadband halogen Light Source. The legend notation is number of line followed by letter indicating column of the position of the patches in the colorimetric chart.

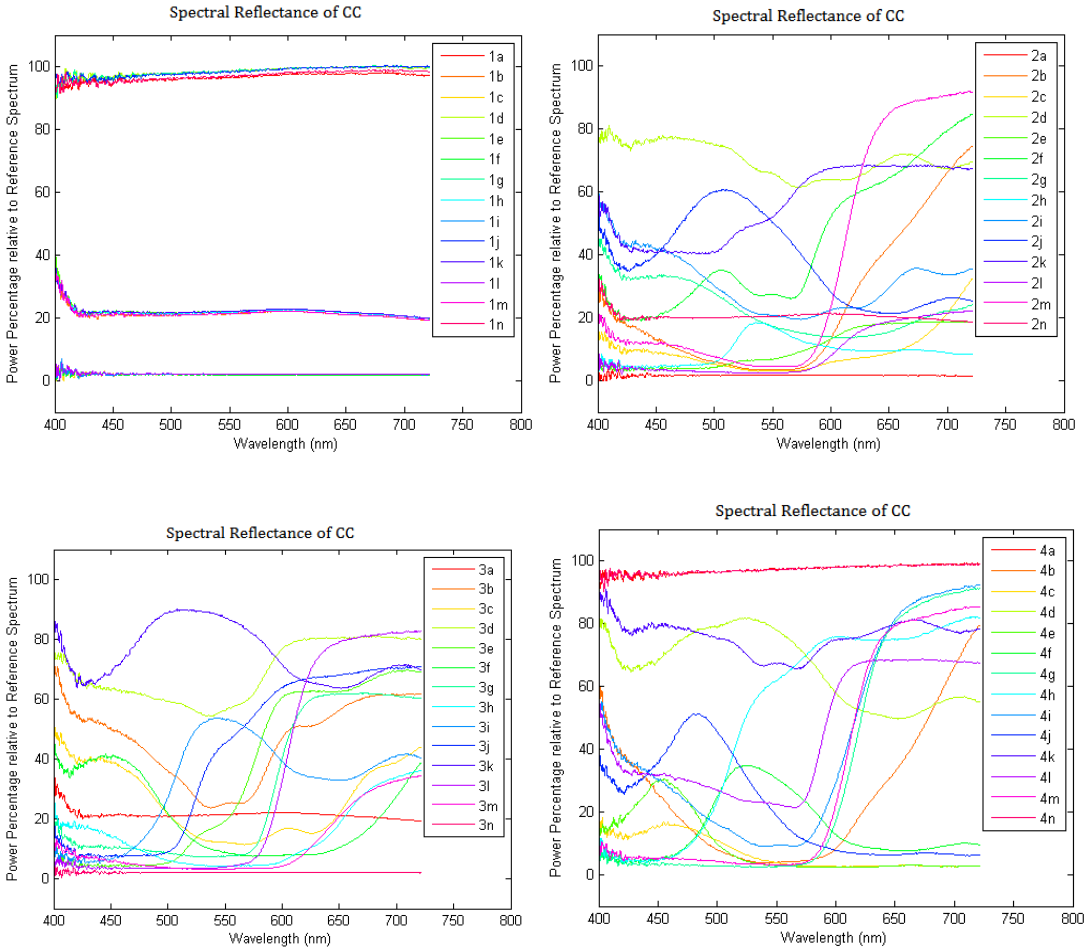

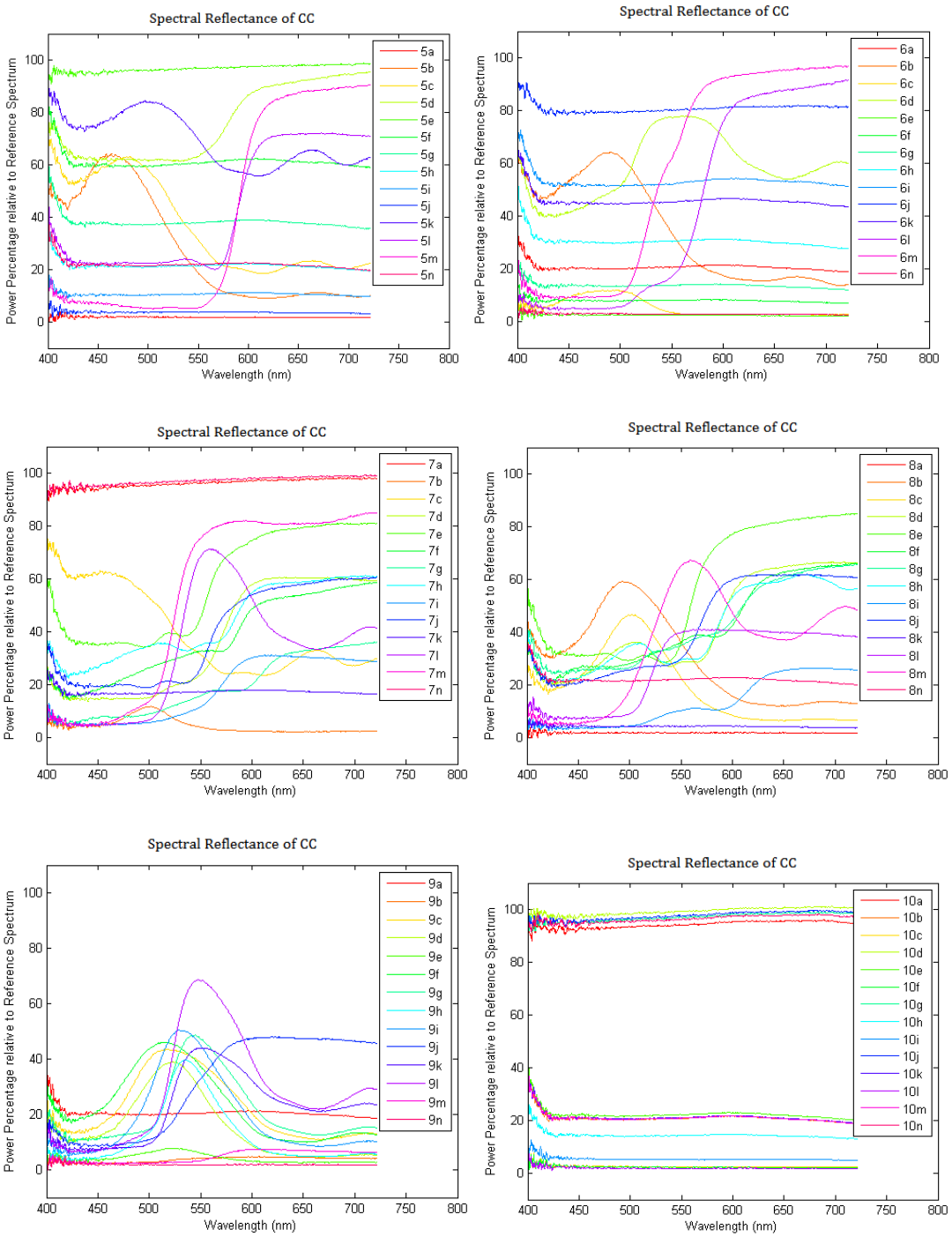

Fig.28: Spectral Reflectances of the 140 colored patches of Xrite SG colorimetric chart. Measured with a halogen source Reference, with a low emission near 400nm which explains the noisy fluctuations at that part of the spectrum. Each of the 10 plots contains the reflectances of 14 patches per line of the chart.

Spectral reflectance that was measured for a Halogen source, a white LED source, and Sunlight was evaluated. Since those sources cover all or almost all of the visible spectrum and do not have significant fluctuations , the recovered spectral reflectances were expected to be almost identical. Color was reproduced for standard illuminant D65 and 2 degrees standard observer CIE 31 with 3 samples at the peaks of the tristimulus curves (445nm,555nm,600nm). The Delta E of the resulting colors was measured in pairs of the corresponding light sources.

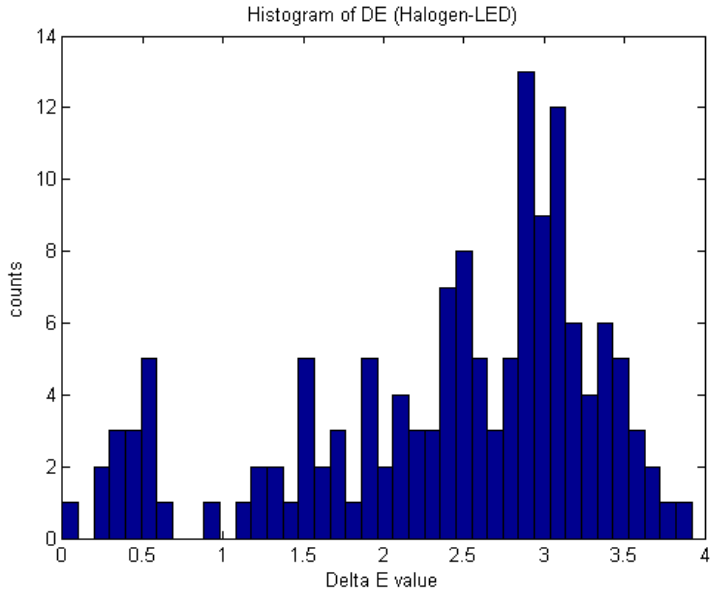

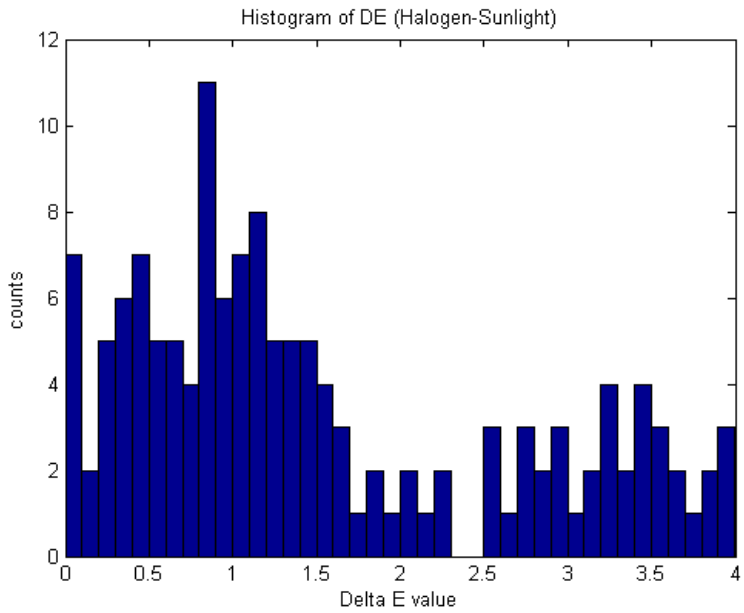

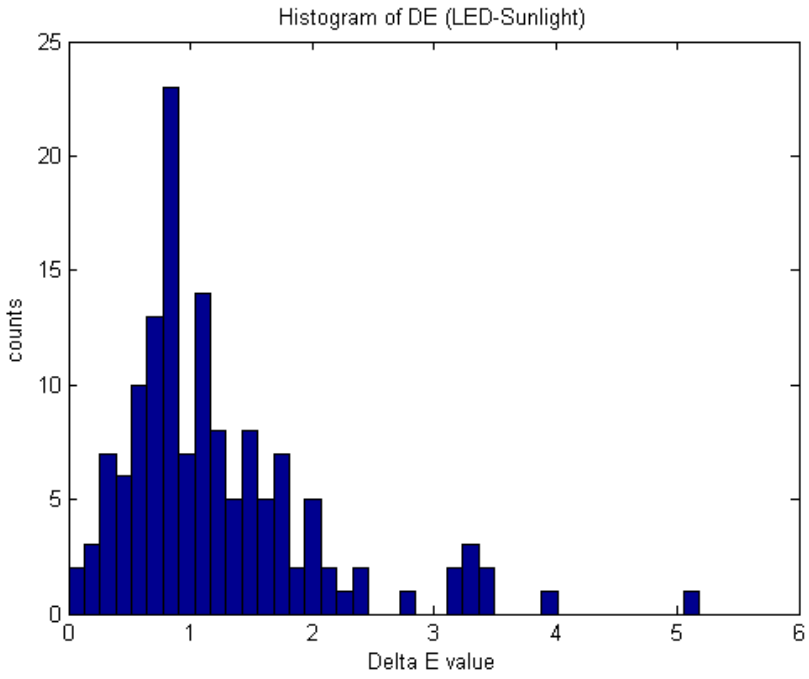

Fig.29: Histograms of the Delta E values, comparing 3 pairs of color sets reproduced from spectral reflectances measured under 3 broadband light sources.

Delta E	Halogen-LED	Halogen-Sunlight	LED-Sunlight
Max	3.8422	3.9984	5.1843
Mean	2.3940	2.1591	1.2298

The comparison of the 3 resulting color sets based on their chromatic difference is analogous to the comparison of the 3 sets of spectral reflectances, since the reproduction was carried under the same conditions. Delta E is quite low -in many cases below the Noticeable threshold- which verifies our original expectations that spectral reflectances recovered should be very close. The difference is greater in the pairs of Halogen-LED and Halogen-Sunlight probably due to the low emission of the halogen source in the lower part of the spectrum.

Small differences can also be attributed to the imperfect nature of the experiment and measurements such as the electric noise, the position and angle of the spectrometer's optic fiber , small imperfections on the chart's surface etc.

Spectral Power Distribution of various Light sources.

The Spectral Power Distribution of 8 light sources was measured. They can be used as a reference in a look up table or database for illuminant estimation, as well as for color reproduction needs. Each curve contains the spectral power data normalized by the maximum value of each source. This can be useful for an overall evaluation of the SPD, as well as a qualitative comparison between different light sources, that allows us to deduce rules for determining the presence of a type of source, in an unknown illuminant scene, by comparing the spectral content.

Sunlight

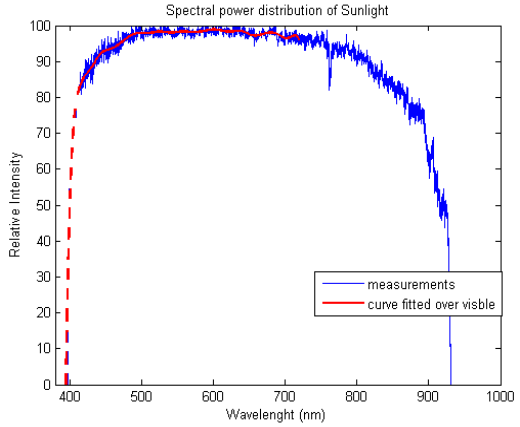

Tungsten Filament Incandescent bulb

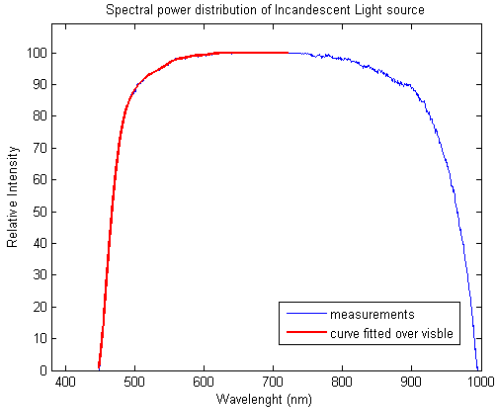

Domestic Halogen bulb

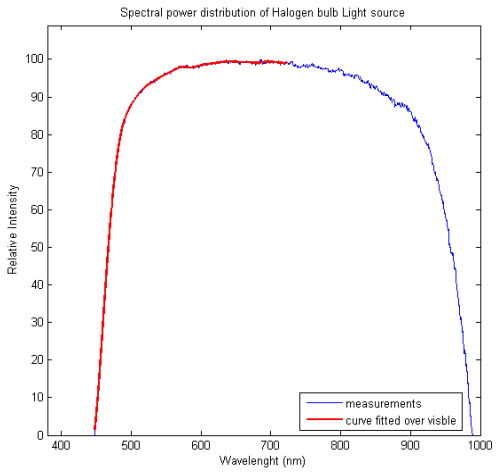

White LED

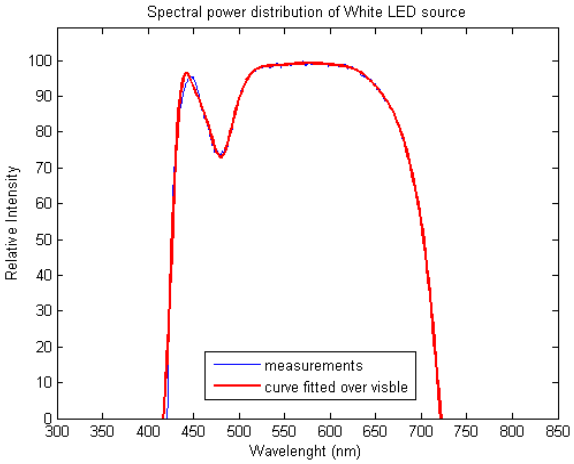

Thor labs OSL1 Halogen thor

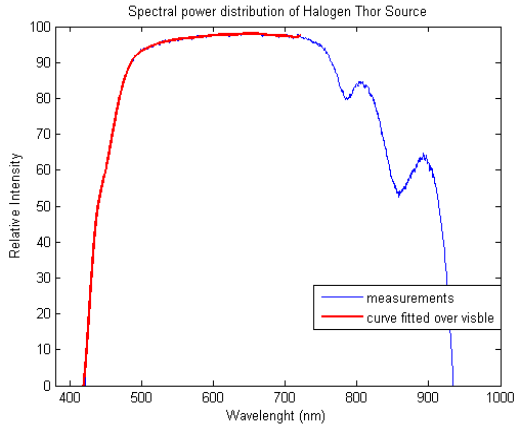

Arkon Photographic Lamps(halogen)

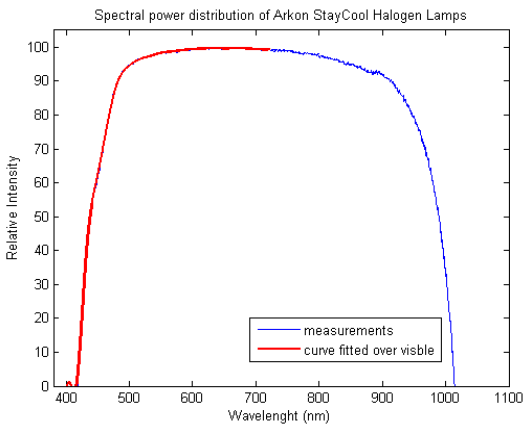

Fluorescent tube 1

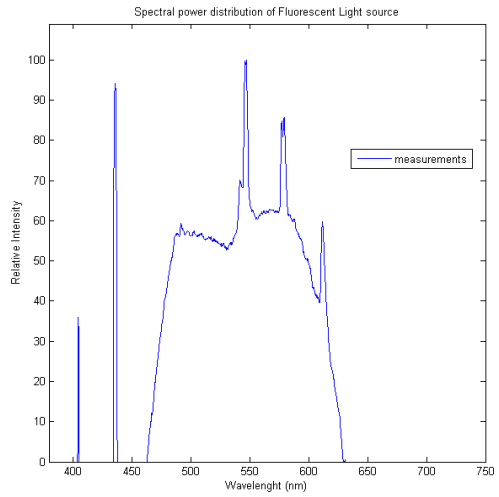

Fluorescent tube 2

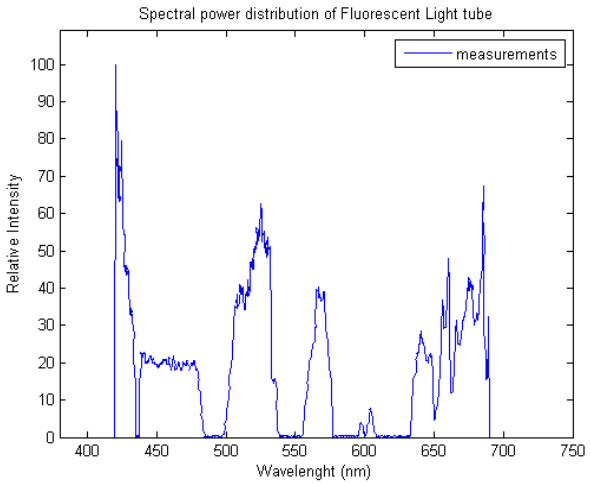

Fig 30: Spectral power Distribution of measured Light sources as a normalized percentage of their corresponding maximum value. To clear the signals of unwanted noisy fluctuations there has been a curve fitting over the visible spectrum in the cases where it was possible. The dash line in the sunlight plot is there to remind us that the SPD of the sun is not actually dropping to zero at around 400 nm but that measurement is rather the inability of the spectrometer used to 'read' below certain wavelengths.

Notice the noisy measurement of sunlight, indicating the difficulty of obtaining a clear spectrometric measurement in real varying conditions. The measurement of the white led is revealing of its characteristic spike in the blue region of the spectrum, while the fluorescent lamps have a rather spiky profile that can be attributed to the different vapor - gas discharges producing light inside the tubes.

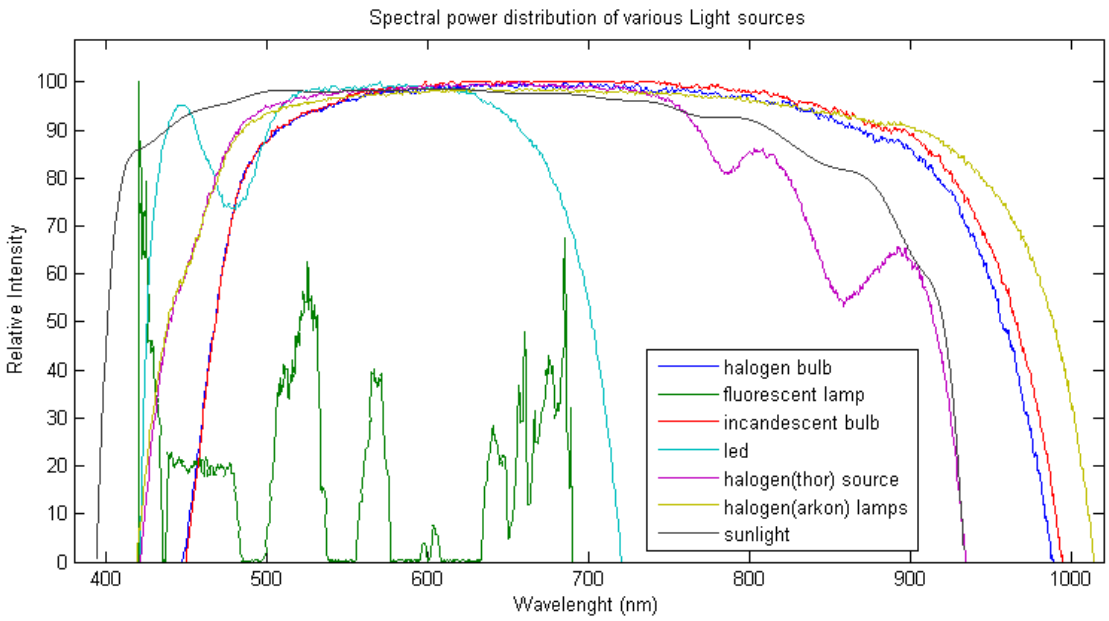

Fig.31: SPD of all light sources measured, combined in a single graph for easier qualitative comparison.

The Figure above combines the curves of all the illumination sources measured, physical or artificial, domestic and scientific, and it allows better understanding of their relative profiles. We can use such information to decide on rules that would allow easy illuminant detection in cases where the source is unknown, by comparing it to a total of other known light sources and concluding about its nature based on its spectral content. For example: We know for a fact that LED or camera flash lights, are not emitting infra red light, so we can exclude them in a case where IR is present in the scene. Furthermore using the starting and ending points of the emission as well as intermediate characteristic ratios we can narrow our choices moreover and finally estimate or even detect the present unknown illuminant.

Color Reproduction of Xrite Color Checker SG 140

Using the Spectral Reflectances and the various Light source curves that we measured we proceed to reproduce the Chart's patches' colors.

Since color fidelity and quality is depended on the sampling rate, or the choice of spectral bands, we compared the results of the reproduction in cases with different number of bands.

Color was reproduced for:

- 3 bands (445nm, 555nm, 600nm, the peaks of the tristimulus curves)
- 6 bands (460, 480, 540, 580, 640, 680 nm, which are the bands our physical multispectral imaging system utilizes).
- 9 bands (445 , 460, 480, 540, 555, 580, 600, 640, 680 nm a combination of the two previous cases)
- 13 bands(from 400 nm to 700 nm with an interval step of 25 nm)
- 16 bands(from 400 nm to 700 nm with an interval step of 20 nm)

We have already shown that with 16 bands we achieve reproduction almost "just as good" as having the continuous full spectrum available so there was no need for higher spectral resolutions. An increased number of bands means greater system complexity, more data to process, analyze and use and thus means greater time to produce results. For that reason, the elapsed algorithm runtimes of the above methods were measured and used for comparison.

Delta E	3 bands	6 bands	9 bands	13 bands	16 bands
Max	66.7697	26.6407	38.2806	2.5032	2.8819
Mean	21.7704	12.0045	12.1766	0.5320	0.8564

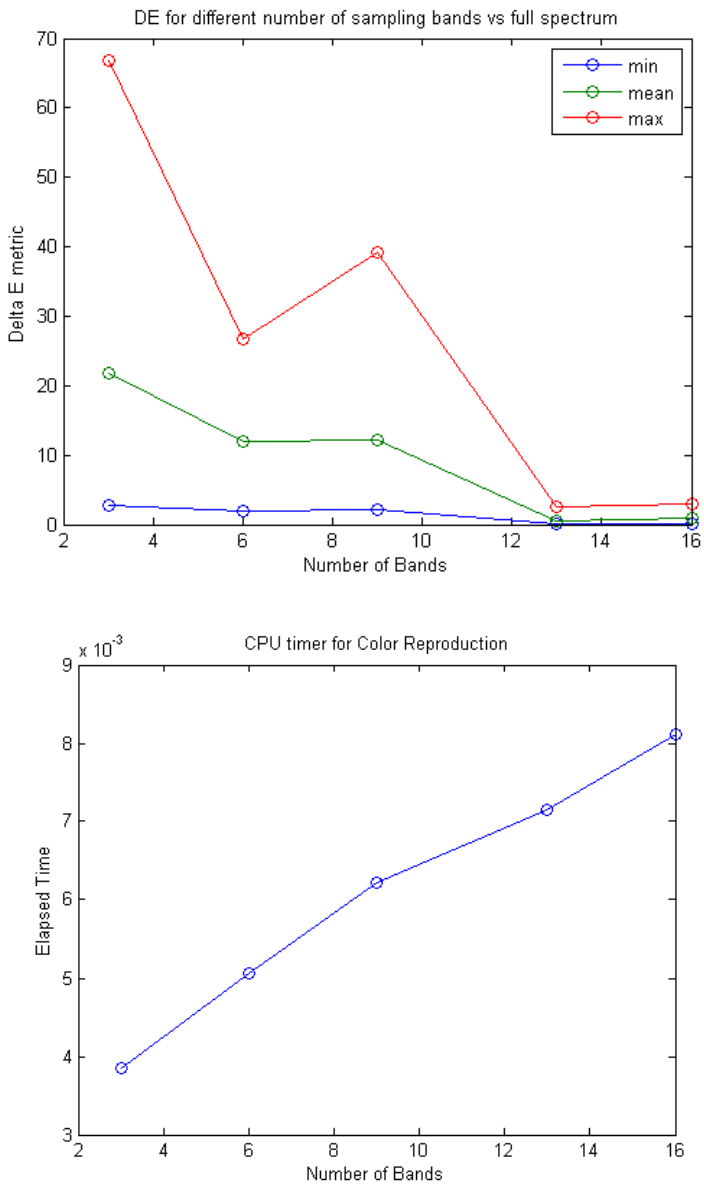

Fig.32: a) Delta E of colors reproduced with different number of spectral bands compared to the ones reproduced from a continuous full spectrum(301 samples, one at each wavelength). b)The CPU timings(in milliseconds) to process the spectral data and produce color for those bands.

The results of the first graph are quite interesting. Delta E drops dramatically with the use of more spectral bands. Even with the use of 13 spectral bands we have results that should be indistinguishable from the full spectrum ones. Only exception is the case of 9 bands that does not seem to follow the same linear behavior. That can be probably attributed to the fact that the bands chosen are not equidistant, and some intervals are greater than others. The time needed to process the data follows a linear ascending manner.

Color Reproduction of CC140 under different illuminants

We present the reproduced color for continuous full spectrum using measured spectral reflectances, for 7 measured light sources and 1 theoretical source(Equal Energy radiator). The spectral sensitivities of the CIE 31 standard colorimetric observer, have been applied.

Sunlight

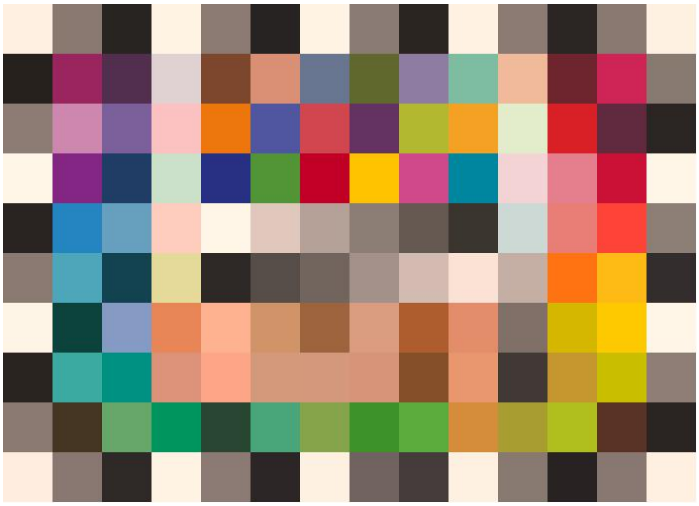

White LED

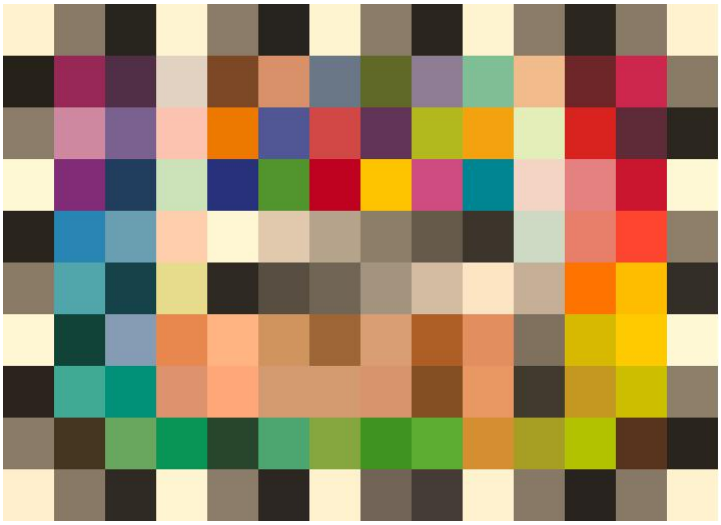

Arkon Photographic Lamps (halogen) source

Thor Labs OSL1 halogen Light

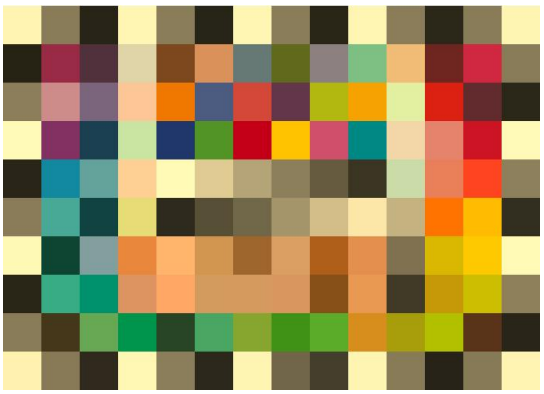

Domestic halogen Light bulb Bulb

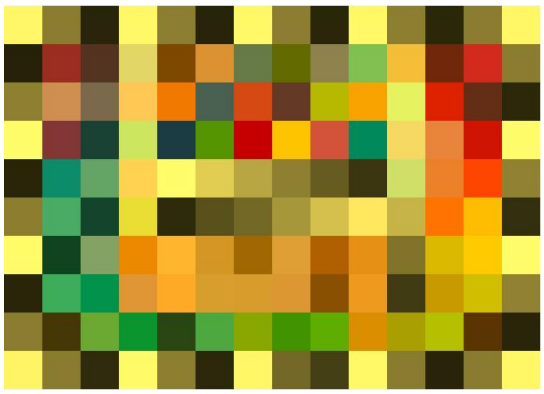

Domestic Incandescent Tungsten

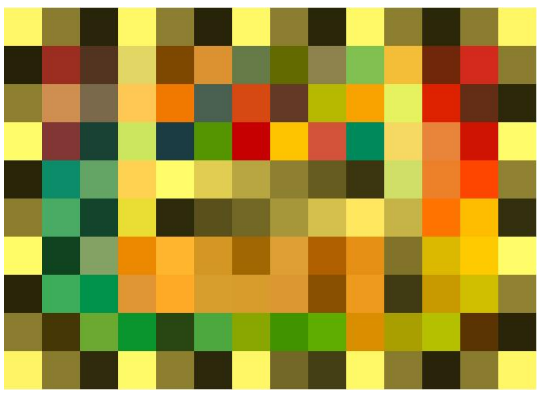

Domestic Fluorescent Tube Source

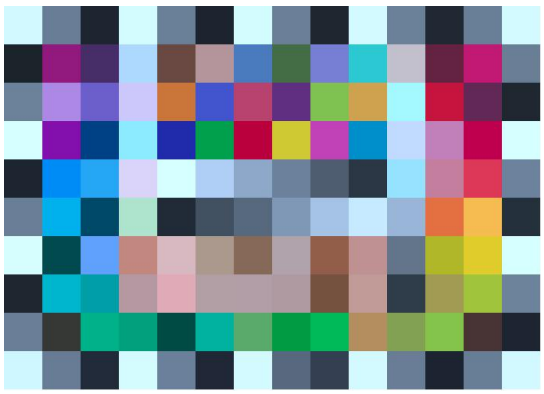

Theoretical Equal Energy

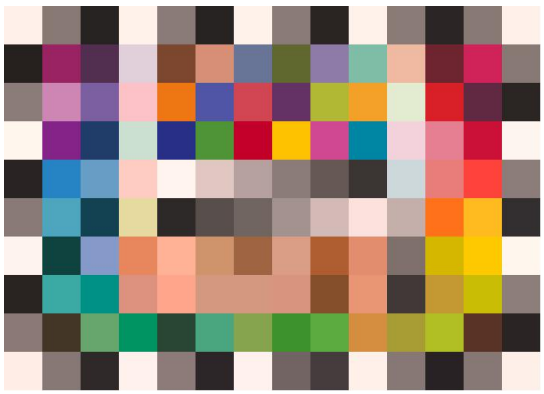

Fig.33: Xrite Color Checker Reproduced Color for various light sources.

Color reproduction of Spectral Cube Data

We reproduced color from various sets of monochromatic spectral Images. Those images were taken with the use of Music Hyper Spectral camera presented in the work of Iliou [10], and their intensities .

Sixteen patches of the Macbeth Color Checker are depicted in sets of four each time. Each spectral cube contains 6 narrow complementary spectral bands centered at 460 ,480 540,580,640,690 nm. The reproduction was carried out for all of our measured light sources and considering both the cases of the 2 degree observer(CIE31) and the 10 degree observer(CIE64).

We started with the four spectral cubes presented below along with the corresponding color image of the point of interest.

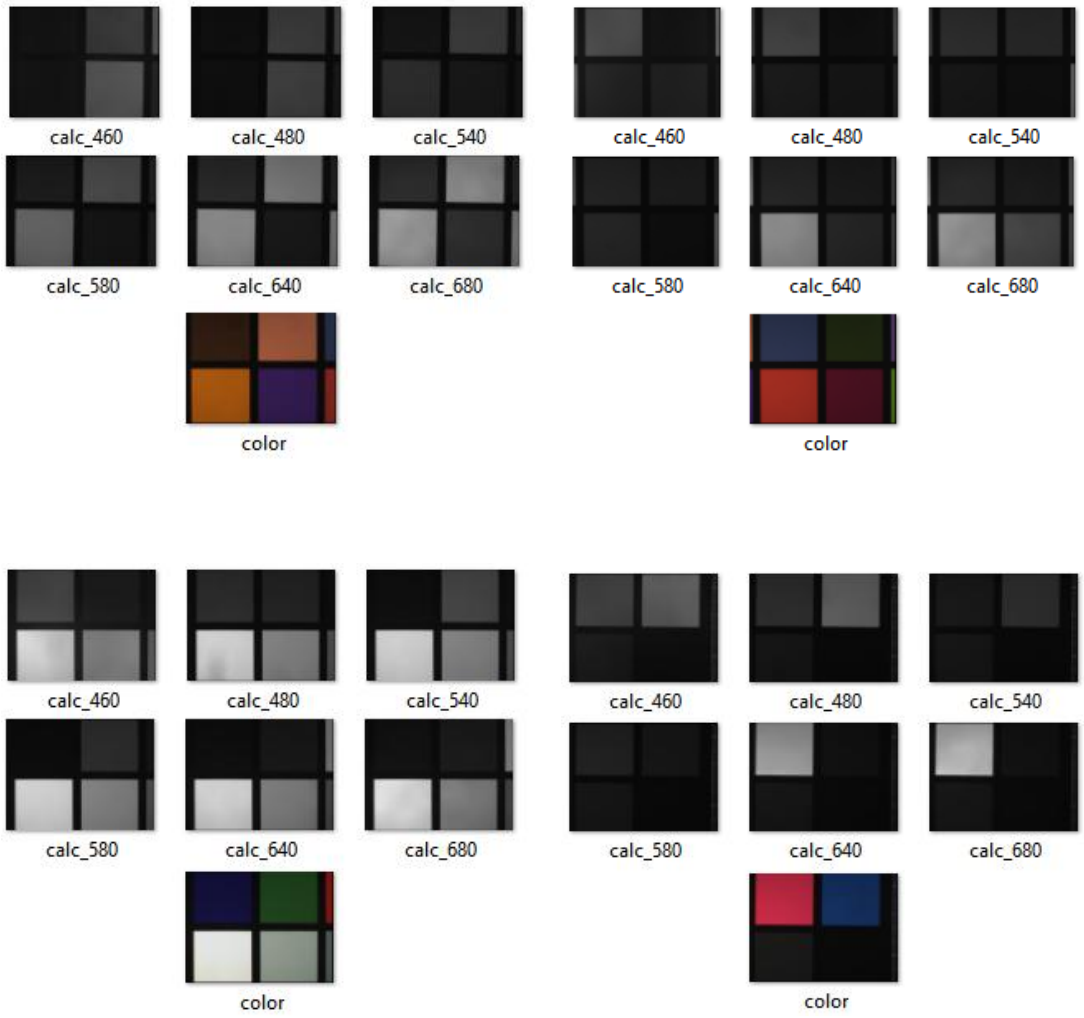

Fig.34: Spectral cube data of 16 CC patches, centered at the registered wavelengths.

The reproduced color images for the 8 types of light source and the 2 different standard observers are presented below. For **standard observer CIE31** :

Set1

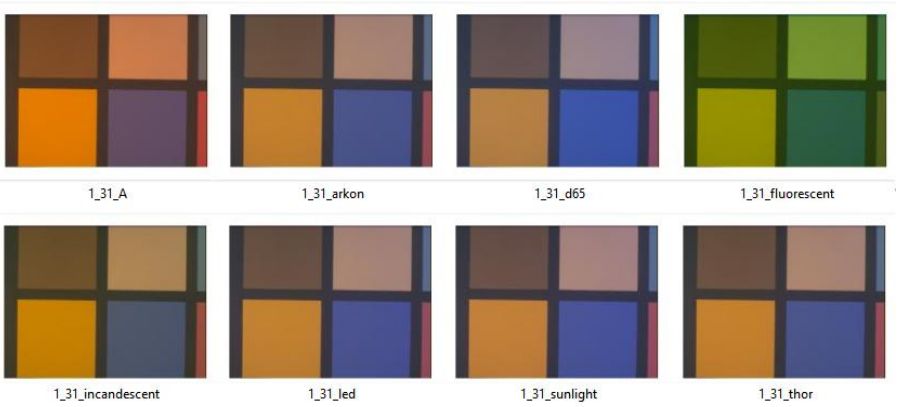

Set2

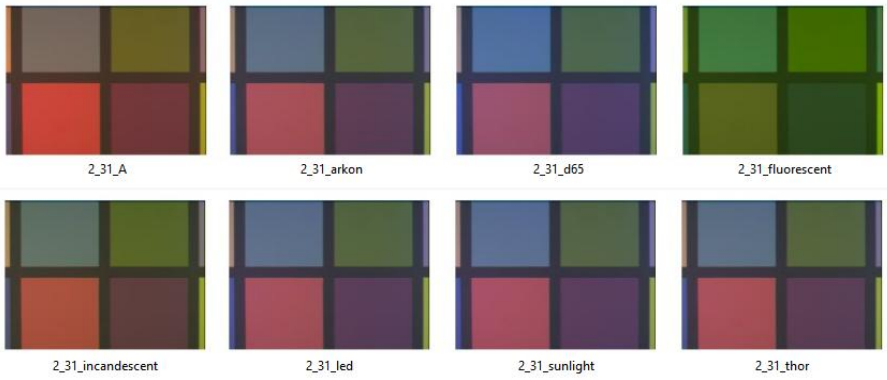

Set3

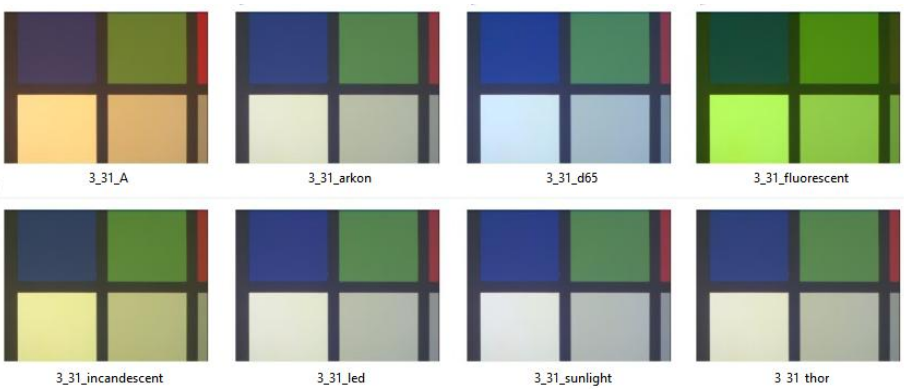

Set4

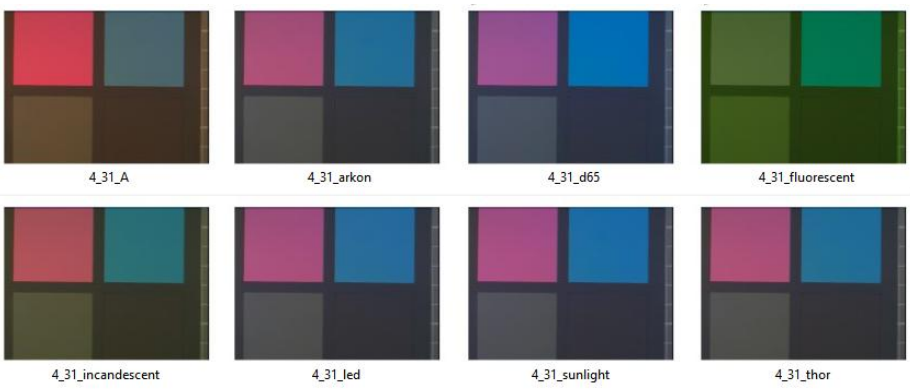

For **standard observer CIE64**

Set1 **Set2**

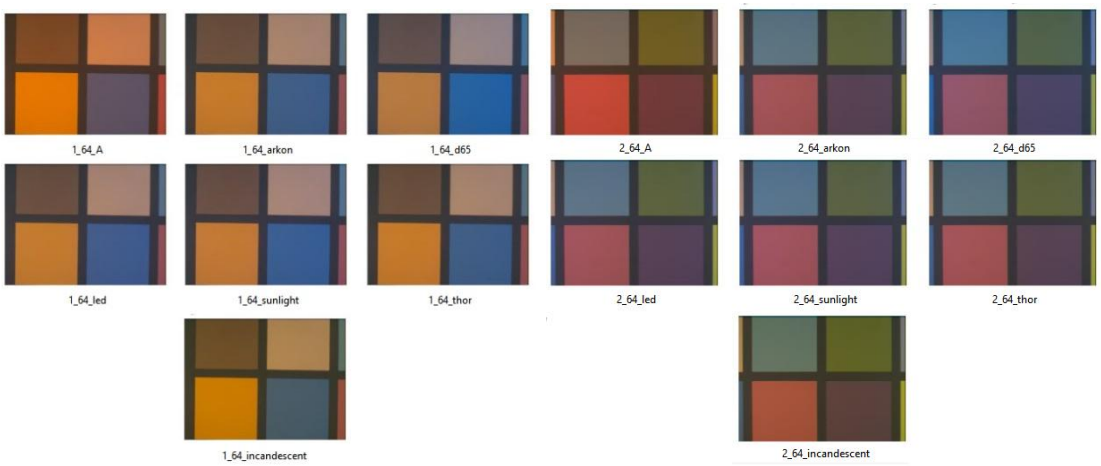

Set3 **Set4**

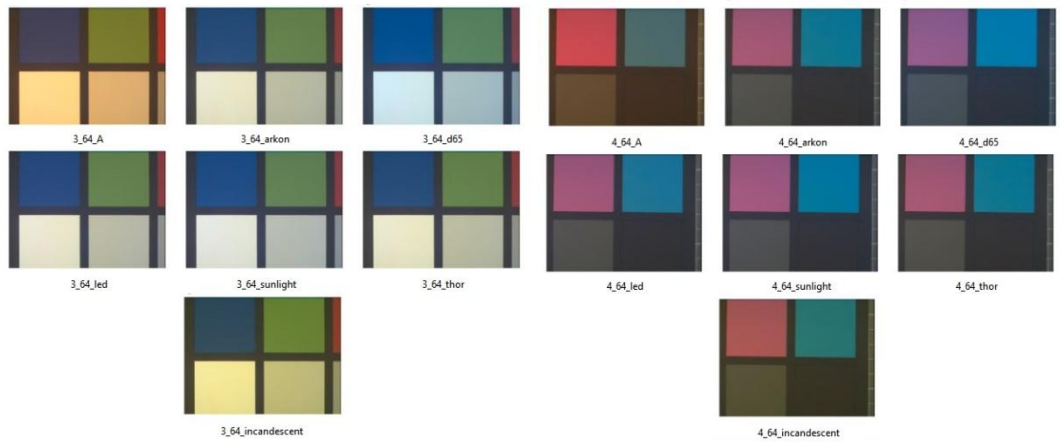

Fig.35: Color Reproduced Images from calibrated Spectral Cube data acquired with the Musis HyperSpectral Imager.

The problematic case of Fluorescent Light Reproduction

Fig.36: Reconstructed images for white led(left) and two fluorescent light sources (center and right)

While we manage to reconstruct images with high color quality the method seems to fail in the cases of fluorescent lights. This is due to the non uniform distribution of their spectral power and the intense spikes apparent in their curves. While the whole range of the lights spectra, that passes through the optical filters, contributes to the amount of photons that the sensor records, when the source is sampled at the center points of the filters the value obtained might not representative of the overall contribution in the region.

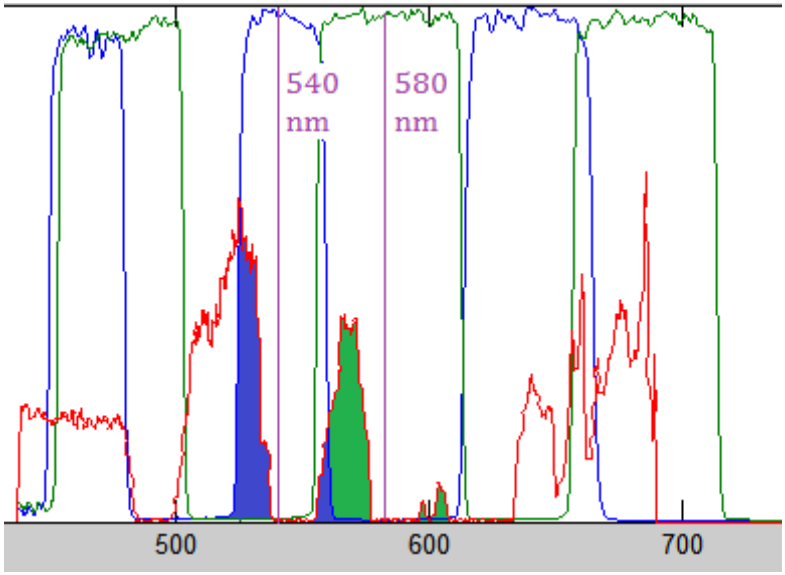

Fig.37 :Concurrent plot of the TBP filters and the fluorescent spectral distribution over their wavelength range.

Consider the Figure above. While there is plenty of light that passes through the optical filters and will eventually be recorded by the CMOS pixels(blue and green regions), due to the high non-uniformity of the fluorescent source in those regions, the value that will be sampled at the center of the filters(noted with purple vertical lines) will be nearly zero resulting in a dramatically distorted pixel chromaticity.

To address this problem we might need to employ different sampling methods, or a higher number of bands.

True Color Image capture and formation.

Using Spectral Cubes (with 6 lambda images each),captured with the Six band Multispectral Snapshot Imager , where the cross-talking of the sensor channels has been cleared out we are able to reconstruct true color images for any required illumination or observer sensitivity.

An example image of a canvas painting initially illuminated with a halogen light source, follows. Its colors have been reconstructed for many different light sources with high color fidelity.

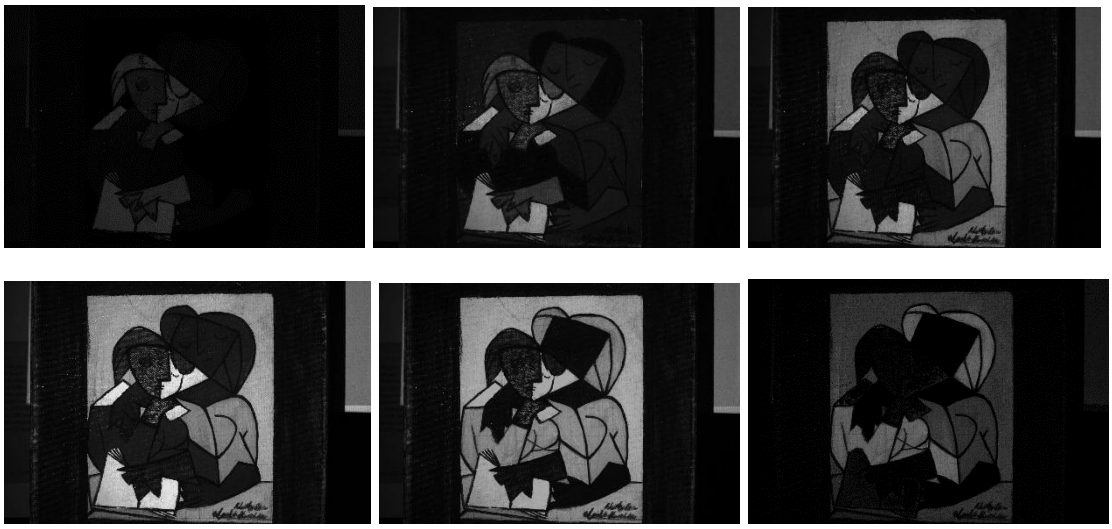

Fig.39: The Spectral cube images of the scene as captured by the Six Narrow Band Multispectral system and after the channel cross-talking has been cleared.

Fig.40. The resulting image produced with the ground truth illuminant.

Fig.41: The canvas image reconstructed for: Measured Sunlight (top left). Standard illuminant D65-sunlight simulator(top right),Measured Incandescent bulb light(bottom left) Standard illuminant A-tungsten filament incandescent light simulator(bottom right).

The mean time for Color production and image formation was for most cases around 0.6 second meaning that the method is ideal for real time spectral imaging.

Determining the Ground Truth illuminant

If we consider real life situations, it is not always possible to know the illumination of the scene and thus the reference with which we will divide our pixel values to extract the spectral reflectance information. For this reason even in our controlled environment and image capture conditions we assumed that the illumination was unknown. To be able to determine or approach it we used a maximally reflective surface(as described previously) usually a piece of white paper, which we captured in the same way we would proceed to capture the scene. An additional exposure was thus needed since generally it cannot be assumed that such a surface will exist in a typical scene.

Besides the six images of the object lambda stack we thus have an additional six for the stack of the white surface images. The brightest of the non saturated pixels represent the light sources intensity at the wavelength of each image.

We originally tried to divide each scene's pixel with the corresponding pixel of the white surface images for the same wavelength, a method that is bound to fail if the white surface is not totally flat and correctly aligned with the camera. Also we would have to make sure that the white surface covers the whole of the camera's field of view.

Fig.42: An unsuccessful attempt at 'per-pixel-division' of the captured scene with the illuminant values obtained through a camera exposure at a maximally reflective surface(white paper). Notice the different colored 'stains' at the left of the image cause by a small incurvation of the paper.

To address this problem we decided to use a single pixel-matrix value per white image, to represent the illuminations intensity. Four different methods were used in order to find the most fitting pixel-matrix to use as a divisor.

- Find the pixel with the highest value in every image, independently of position(prone to error of saturated pixels)
- Find the brightest pixel in the brightest image and use it together with all the pixels of the same x,y coordinates in the lambda dimension.
- Find the brightest pixel in the brightest image and use it together with all the pixels of the same x,y coordinates in the lambda dimension.
- Find the brightest pixel in every image and use the ones with the maximum monotony as a function of wavelength.

The last one is less prone to error since most of the light sources we used were quite broadband and with no significant spikes(beside fluorescent) meaning they were quite monotonous in wide wavelength ranges as well.

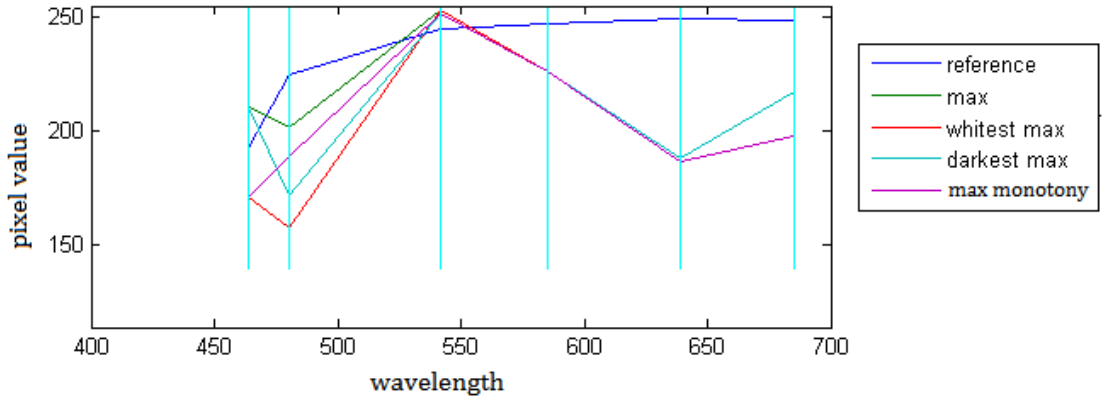

Fig.43: Example of the 4 different methods used to find the reference divisor. The vertical cyan lines represent the points of sampling, a single image each.

Fig.44: Resulting images after the division with the four pixel-matrixes. From top left to bottom right: Max, Brightest Max, Darkest Max, Max monotony.

Metamerism. - Color Reproduction of Metameric Grays

While color imaging systems suffer from the phenomenon of metamerism, spectral imaging systems provide a solution to it, since the depicted object or scene becomes independent of illumination and observer conditions.

To prove this point we reproduced the color of twelve metameric grays under various illuminations, and with different number of bands. The grays' spectra come from the Color Science[3] book and are a characteristic example of how severe the phenomenon of metamerism can be under certain conditions. The twelve grays are a metameric match under illuminant D65, but when shifting the light towards a lower temperature it becomes apparent that they mismatch dramatically.

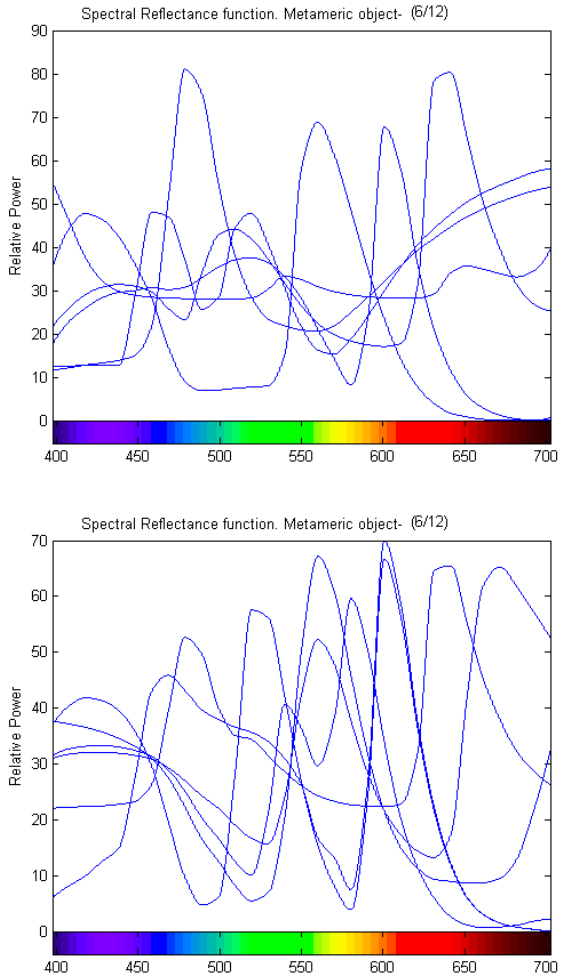

Fig.45: Spectral Reflectances of 12 surfaces that appear grey under illuminant D65 when viewed from CIE1931 standard observer.

Notice how different the curves are from each other. Yet those totally different surfaces yield the same color under certain (very common ,daylight) conditions. The apparent color of those surfaces was produced with a use of

31 bands in total.

Fig.46: The twelve metameric surfaces in full metameric match condition. When viewed under illuminant D65 all twelve surfaces appear the same color and thus appear as one.

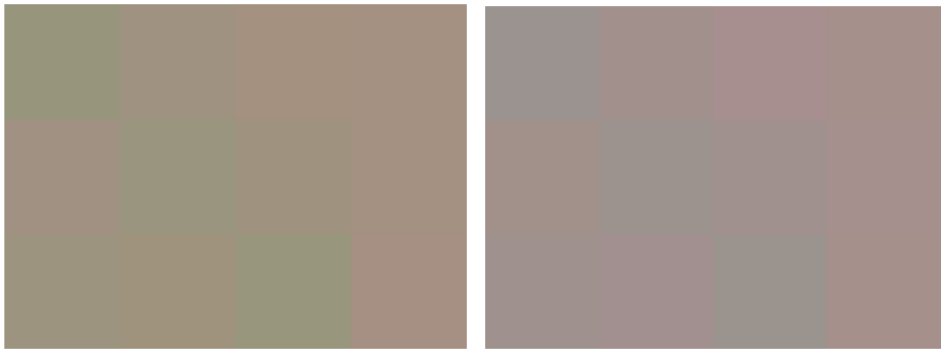

Fig.47: The surfaces under illuminants D50(left) and E(right). Even with small changes in illumination the shifting of the color and the mismatch are apparent. With an even more drastic change, such as illuminant (below) the mismatch of all twelve patches is clear.

The Delta E of those patches was measured against the color they had under their metameric match condition.

Color with D65

X	Y	Z	L	a	b
28.484	30.000	32.615	61.6542	-1.71	-12.89

31 Samples method				
Delta E	D65	D50	E	A
max	0	15,468013375	9,3347727364	52,590807901
mean	0	13,274402206	7,0703043693	49,380000993
min	0	11,564492369	3,4816026836	47,057524468

The surfaces were reproduced with the 6 narrow band method as well. As stated before metamerism occurs when the integrals of two color signals with the observers color matching function are equal, or that they are somewhat "symmetric" under that curve. The 6 bands method breaks that condition(or that symmetry) and is thus able to reveal the difference in chromaticity between two metamers.

6 bands method				
Delta E	D65	D50	E	A
max	45,832302461	41,645148280	39,553910719	57,739338759
mean	22,868146282	20,286413703	20,247939043	40,107332681
min	5,1280236833	2,2039492478	1,9609011753	21,887177981

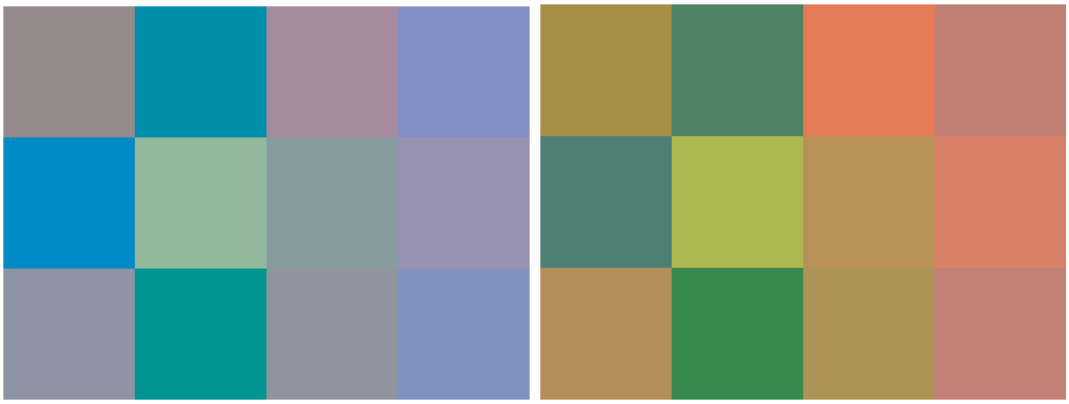

Fig.48: Color reproduction of the 12 metameric grays for the 6 narrow band method, with illuminants D65 on the left (initial metameric condition) and illuminant A on the right(severe mismatch).

The method appears to be free of metamerism instances, but we can notice significant chromatic difference, even in the case where colors originally appeared the same. In such cases, if color fidelity is considered more important the use of spectral estimation algorithms and a higher sampling rate is recommended.

Future Work

The True Color Formation Flowchart presented in section 1 shows that Color Reproduction is used on Spectral Cubes after the various methods of Color Channel Unmixing/ Deconvolution, Illuminant Detection, and Spectral Prediction/ Estimation have been applied on the initial image set. All of the above are areas that need to be addressed with practical and robust solutions to achieve better results.

Multiple illuminant estimation using NIR

The experiments on this thesis were conducted under the hypothesis that one illuminant is present in the scene, something that its not true in most real life imaging situations where the presence of outdoor shadows, office or workplace fluorescent lighting, camera flashes etc make it harder to evaluate the real Spectral Reflectance of objects. Cases of light bulb types with the same white point but different metameric properties are also considered problematic while simple solutions like the grey ball and gray world algorithm[22][23] or a maximally reflective surface[24] seem insufficient to tackle them.[25]

The problem of many illuminants is considered an ill-posed problem. Consider a simple Bayer filtered RGB camera. For a given image of n pixels (or n depicted surfaces) we have only 3x n known values(RGB vectors) at our disposal while trying to solve for 3x n(unknown reflectances) + 3 additional values that correspond to the illuminant. The same problem principle carries on to more complex and detailed solutions regardless of the number of spectral bands used.[26]

A very promising solution seems to lie in the use of near infra red information if we notice that almost no surface besides water has higher NIR than visible reflectance, and that NIR is relatively color transparent. Thus it can be concluded that if NIR intensity is lower than visible intensity then the illuminant is the predominant factor in the evaluation of reflectance. Additionally if we consider that most sources(with the exception of LED, flash or fluorescent) follow the behavior of the Plancian black body, and thus are monotonic in the infra red region. Given the above properties of NIR we can conclude that the use of a per pixel basis ratio for visible vs NIR can be extremelly helpful to determine the illuminants present in the scene.[27]

$$V_R = \frac{R}{NIR};\ V_G = \frac{G}{NIR};\ V_B = \frac{B}{NIR}$$

Ratios of RGB values vs NIR value.

The use of NIR allows us for more accurate estimation since we can practically double the spectral bandwidth of control (distance to visible up to 400nm), and have more relevant results since the initial information is less correlated.

The NIR information can be acquired with an additional camera, or an additional snapshot where we take advantage of the leak present in one of the triple band pass filters in the infrared region.

Field work and image dataset

To further test our system, methods and algorithms the creation of a large image dataset of different objects captured under various conditions is required. A hands-on field work approach is demanded to test the practicality, speed and robustness of the system. A large collection of images can be amassed which then can be used for Spectral Clustering, Material Classification and evaluation of various surfaces metameric properties (both naturally occurring and artificial or human made).

Spectral Rendering

The methods and algorithms used for Spectral Color Reproduction could be implanted as a plug-in to be incorporated into major design programs for the needs of spectral rendering. The scene's light transport can be modeled in wavelengths. Its emission spectrum can be set to release photons at a specific wavelength in proportion to the spectrum (to model monochromatic or ambient light) and the objects' spectral reflectance curves can be similarly used to more accurately represent it. The real color of objects under varying lighting conditions and viewing angles can be produced and rendered into any design with a small tradeoff of computing complexity and time in an already resource and time intensive procedure.

Conclusion

Throughout this thesis, we studied methods for proper color reproduction from spectral data. The spectral Reflectance of multiple chromatic patches, and scenes was acquired and their color produced under a variety of light sources that we had measured and categorized. We showed that twelve to sixteen spectral samples are more than enough to reproduce color that's indistinguishable from the real one. A practical six narrow band multispectral system is used for real time color reproduction and imaging. Finally, the phenomenon of metamerism, a perceptual problem, is addressed and the real chromatic relationship between metameric groups revealed.

Color, we could say, is a universal language. It affects and shapes the lives of all of us. Color constancy and high color fidelity are two qualities required in numerous activities and crucial for many industries. Spectral Imaging, and practical applications of it more so, is a powerful tool that addresses those topics and help us bridge the gap between the natural world and human perception.

Bibliography

References

[1]Berlin, B. and Kay, P., Basic Color Terms: Their Universality and Evolution, Berkeley: University of California Press, 1969.

[2] Waldman, Gary (2002). Introduction to light: the physics of light, vision, and color (Dover ed.). Mineola: Dover Publications.

[3] Wyszecki and Stiles 1982 : Color Science Concepts and Methods, Quantitative Data and Formulae.

[4] Judd, Deane B.; Wyszecki, Günter (1975). Color in Business, Science and Industry. Wiley Series in Pure and Applied Optics (third ed.).

[5] Leong, Jennifer. "Number of Colors Distinguishable by the Human Eye" hypertextbook.com

[6] IUPAC, Compendium of Chemical Terminology, 2nd ed. "Reflectance".

[7] CIE International Lighting Vocabulary

[8] D. Iliou Diploma Thesis Spectral Prediction From Filtered Color CCD Cameras Technical University of Crete

[9] D. Iliou Msc Thesis Hyper Spectral Data Estimation from Power Dimensionality Experimental Imaging Technical University of Crete

[10] David H. Foster ,Kinjiro Amano Frequency of metamerism in natural scenes.

[11] "OSA – Basic slit spectroscope reveals three-dimensional scenes through diagonal slices of hyperspectral cubes

[12] B. Grusche Hyperspectral imaging with spatiospectral images from a simple spectroscope - Basic slit spectroscope reveals three-dimensional scenes through diagonal slices of hyperspectral cubes -

[13] J. Parkkinen and T. Jaaskelainen "Characteristic spectra of munsell colors", Journal of The Optical Scociety of America

[14] Roy S. Berns and Lawrence A. Taplin (2006). "Practical Spectral Imaging Using a Color-Filter Array Digital Camera"

[15] Ocean Optics USB4000 Spectrometer Operation Files

[16] Performing Photometric & Colorimetric Measurements of Light Sources - Robert Yeo Pro-lite Technology

[17] Michael Stokes; Matthew Anderson; Srinivasan Chandrasekar; Ricardo Motta 1996. "A Standard Default Color Space for the Internet – sRGB,

[18] "CIE 1976 L*a*b* Colour space draft standard"

[19] "Delta E: The Color Difference". Colorwiki.com

[20] Lindbloom, Bruce Justin. "Delta E (CIE 1976)". Brucelindbloom.com.

[21] Gaurav Sharma (2003). Digital Color Imaging Handbook. CRC Press.

[22] Buchsbaum G. 1980. A spatial processor model for object colour perception.Journal of The Franklin Institute

[23] Gershon R., Jepson, A. D.,and Tsotsos, J. K. 1987.From [r, g, b] to surface reflectance:, Computing color constant descriptors in images. In International Joint Conference on Artificial Intelligence.

[24] Barnard, K., Martin, L., Funt, B.,and Coath, A. 2002. A data set for color research. Color Research & Application.

[25] A study of illuminant estimation and ground truth colors for color constancy Cheng dongliang National university of Singapore 2015

[26] Enhancing the Visible with the Invisible: Exploiting Near-Infrared to Advance Computational Photography and Computer Vision. Sabine Süsstrunk and Clément Fredembach EPFL 2010

[27] Illuminant estimation and detection using near-infrared. Clement Fredembach and Sabine Susstrunk EPFL

[g1] Judd, Deane B.; MacAdam, David L.; Wyszecki, Günter (August 1964). "Spectral Distribution of Typical Daylight as a Function of Correlated Color Temperature"

Appendix

[A1]The reference illuminant white points for the XYZ to LAB conversion are:

For Illuminant D50:	For Illuminant D65
Xn=96.42	Xn=94.04
Yn=100.00	Yn=100.00
Zn=82.51	Zn=108.8

[A2] The Bradford transformation matrix for chromatic adaptation

$$[M_A] = \begin{bmatrix} 0.8951 & 0.2664 & -0.1614 \\ -0.7502 & 1.7135 & 0.0367 \\ 0.0389 & -0.0685 & 1.0296 \end{bmatrix}$$

Glossary

Illuminants In order to determine the chromaticity, or colorfulness, of light color scientists use theoretical sources. These model sources are called blackbodies or Planckian radiators (after Planck's Law, which describes how to determine the spectral power distribution of a light source based on its temperature). The term source is used in color theory to identify a physical source of light, such as a light bulb. For theoretical models, the term used is illuminant.
Light sources, whether actual sources or illuminants, are primarily characterized by their color temperature and spectral power distribution. Standard illuminants are theoretical constructions that characterize the profile of different types of sources of visible light. Illuminant A to represents typical, tungsten-filament lighting, incandescent source. Illuminants D represent natural daylight in various Correlated Color Temperatures. They are normalized according to the value of the SPD at 550 nm [g1].Illuminant E is an equal-energy radiator; with constant spectral power distribution inside the visible spectrum.

Color Temperature Color temperature refers to the heat of a light source. As color temperatures vary, so does the content of the light in terms of the relative power of its integral wavelengths. Color temperature is always measured in Kelvins.

Image Registration Image registration is the process of transforming different sets of data into one coordinate system. Data may be multiple photographs, data from different sensors, times, depths, or viewpoints. Registration is necessary in order to be able to compare or integrate the data obtained from these different measurements.